



Original Paper

Cobalt Prospectivity Using a Conceptual Fuzzy Logic Overlay Method Enhanced with the Mineral Systems Approach

Vesa Nykänen ^{1,2} Tuomo Törmänen,¹ and Tero Niiranen¹

Received 23 March 2023; accepted 13 August 2023

Published online: 31 August 2023

This paper describes mineral prospectivity research conducted in Finland to predict favorable areas for cobalt exploration using the “fuzzy logic overlay” method in a GIS platform and public geodata of the Geological Survey of Finland. Cobalt occurs infrequently as a core product in mineral deposits. Therefore, we decided to construct separate conceptual mineral prospectivity models within the Northern Fennoscandian Shield, Finland, for four deposit types: (1) “*Orthomagmatic Ni–Cu–Co sulfide deposits*,” (2) “*Outokumpu-type mantle peridotite-associated volcanogenic massive sulfide (VMS)-style Cu–Co–Zn–Ni–Ag–Au deposits*,” (3) “*Talvivaara black shale-hosted Ni–Zn–Cu–Co-type deposits*” and (4) “*Kuusamo-type (orogenic gold with atypical metal association) Au–Co–Cu–U–LREE deposits*”. In addition, we created a model combining till geochemical data with data derived from bedrock drilling and mineral indications, including boulders and outcrops. The mineral prospectivity models were statistically tested with the “*receiver operating characteristics*” method using exploration drilling data from known mineral deposits as validation sites. In addition, the predictive performance of the models was evaluated by using success rate curves, where the number of previously identified deposits was compared with the area coverage of the predicted highly favorable areas. These results indicate that the knowledge-driven mineral prospectivity method using parameters derived from mineral systems models is effective in defining favorable exploration target areas at the regional scale. This study’s innovation lies in its comprehension of the process of evaluating mineral prospectivity when the commodity of interest is not the primary commodity within the mineral system.

KEY WORDS: Mineral prospectivity mapping, Fuzzy logic, Mineral systems, Cobalt, Finland.

INTRODUCTION

The vocabulary of mineral prospectivity mapping (MPM) varies in the scientific literature, and it has also been referred to as “*mineral prospectivity analysis*,” “*spatial predictive modeling*,” “*mineral potential modeling*” and “*exploration targeting*” (e.g., Bonham-Carter, 1994; Pan & Harris, 2000;

Carranza, 2008; Porwal & Kreuzer, 2010; Yousefi & Nykänen, 2017; Hronsky & Kreuzer, 2019; Yousefi et al., 2019). Whatever the method is called, its aim is to delineate or highlight areas favorable for mineral exploration using a geographic information system (GIS). By incorporating the “*mineral systems method*” (Knox-Robinson & Wyborn, 1997; McCuaig et al., 2010; Joly et al., 2015; Hagemann et al., 2016) into the modeling, we can include critical parameters related to the formation of mineral deposits in the targeting model by creating mappable proxies for these parameters derived from various exploration-related spatially referenced da-

¹Geological Survey of Finland, P.O. Box 77 96101 Rovaniemi, Finland.

²To whom correspondence should be addressed; e-mail: vesa.nykanen@gtk.fi

tasets. Finally, this information can be integrated into one map emphasizing the most prospective regions for the commodity of importance (Fig. 1). A classical mineral systems model would include: (1) sources for metallic elements or fluids and heat sources; (2) transportation channels or conduits for metalliferous fluids; (3) physical, chemical, mechanical or other types of traps for fluids; (4) deposition of the ore; and (5) the preservation component (McCuaig et al., 2010). In this work, we used a mixture of the derivatives from a classical mineral systems modeling project and a hands-on mineral exploration project. Hronsky and Groves (2008) divided the approaches to target identification into two end-member classes: the hierarchical and Venn diagram systems. We used the Venn diagram approach, in which we recognized zones where several critical constraining factors in the targeting model interconnect. This approach has been applied, for example, by Nykänen et al. (2017) and in most studies using a GIS platform for MPM.

The motivation for conducting mineral prospectivity mapping for cobalt within the whole area of Finland arises from the increasing need for battery metals in the European Union (Horn et al., 2021). Finland refines around 10% of the global refined cobalt output (IEA, 2021) and is the only country within the EU that produces cobalt from domestic mines. According to Horn et al. (2021), the largest cobalt resource in Europe is situated in the Sotkamo (Talvivaara) polymetallic nickel–copper–zinc–cobalt sulfide deposit in Finland. With this study, we aimed to indicate areas where new cobalt-bearing ore deposits have the potential to be found. Exploration activity for cobalt is increasing, and the Fennoscandian Shield has been considered as high-priority terrain for different deposit types also having significant quantities of cobalt (Horn et al., 2021).

As cobalt is rarely the main commodity in an ore deposit, there is no single mineral systems model that could be used to define the critical parameters needed to build the targeting elements for mappable criteria that are used for mineral prospectivity mapping (MPM). It has been estimated that up to 90% of cobalt is manufactured as a by-product of other metals such as nickel and copper, and although some mines produce cobalt as a primary product, the volumes are smaller than for those mines that produce it as a by-product (IEA, 2021). Therefore, we decided to construct four separate mineral systems-based mineral prospectivity maps favorable for dif-

ferent cobalt-bearing mineral deposit types and then finally to combine these into a single cobalt prospectivity map of Finland. We consider this a novel and unique approach that has not previously been used. A traditional mineral systems-based MPM exercise (McCuaig et al., 2010; Hagemann et al., 2016) would concentrate on a single mineral systems model rather than a multiple model combining several different deposit types. For comparison with the mineral systems-based approach, we also constructed a “Co-indications-based” model, which was constructed on exploration drilling and field observations. This is discussed separately below and compared with the combined mineral systems-based mineral prospectivity map. The mineral systems-based models were validated by using the locations of deposits with cobalt resources indicated in the mineral deposit database (Geological Survey of Finland, 2022a). The combined model was validated using exploration drilling sites with assayed samples containing over 500 ppm cobalt. The anomaly model was also validated using assayed samples containing over 500 ppm cobalt, but these were a randomly selected subset from the full dataset, as the same data were also used to build the model.

MINERAL PROSPECTIVITY MAPPING METHOD

State-of-the-art Methods for Mineral Prospectivity Mapping

Mineral prospectivity mapping plays a crucial role in the identification and evaluation of areas with potential mineral resources. Over the years, advancements in technology and data availability have revolutionized the field, leading to the development of state-of-the-art methods for mineral prospectivity mapping.

One key aspect of modern mineral prospectivity mapping is the integration of diverse datasets, including geological, geochemical, geophysical and remote sensing data (Carranza, 2008). Advanced data integration techniques, such as geographic information system (GIS), enable the combination and analysis of heterogeneous data sources (Bonham-Carter, 1994). These methods facilitate the identification of mineralization indicators and the generation of comprehensive prospectivity models.

The application of machine learning (ML) and artificial intelligence (AI) techniques has signifi-

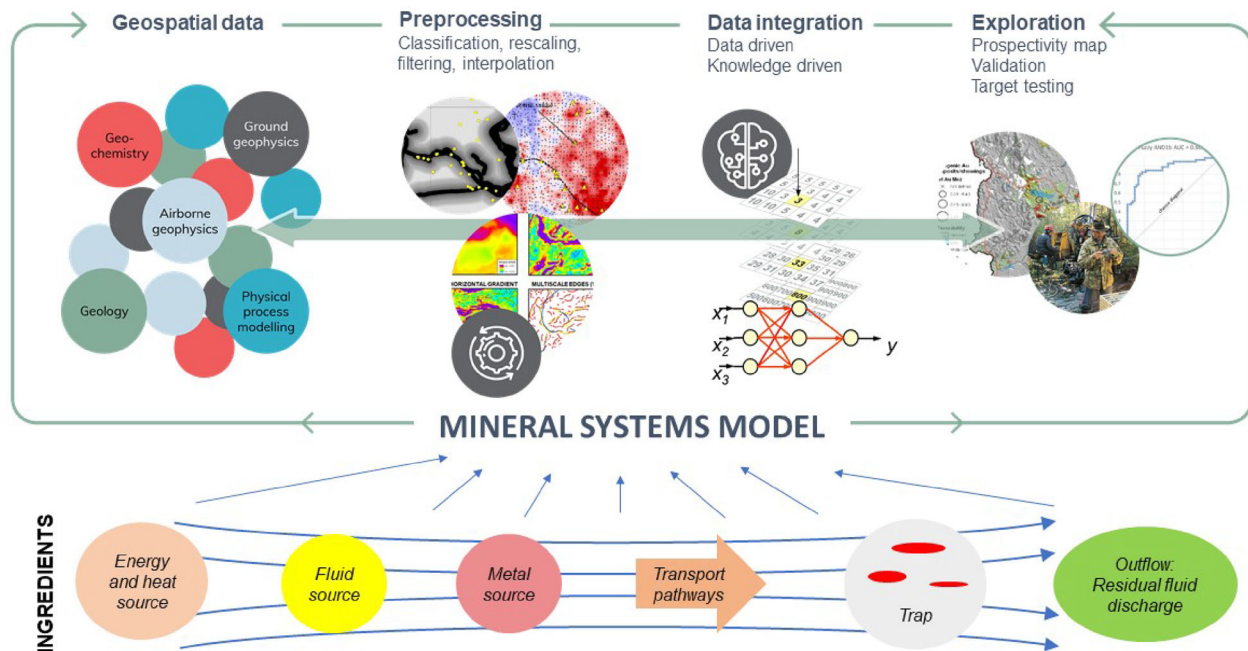


Figure 1. Flowchart describing the components involved in mineral prospectivity mapping (MPM) (Pan & Harris, 2000; Harris & Sanborn-Barrie, 2006; Nykänen et al., 2008a) and mineral systems modeling (MSM) (Knox-Robinson & Wyborn, 1997). MSM is used as input to MPM by providing information on which data are useful for each mineral deposit type.

cantly enhanced mineral prospectivity mapping (Rodríguez-Galiano et al., 2015). ML algorithms, such as random forests (Carranza & Laborte, 2015; Harris & Grunsky, 2015; Carranza & Laborte, 2016), support vector machines (Zuo & Carranza, 2011) and neural networks (Porwal et al., 2003b; Nykänen, 2008), can effectively analyze large datasets and identify complex patterns. These methods enable the extraction of valuable information from geological and geospatial data, leading to accurate mineral potential predictions and the identification of previously unknown mineralization targets.

Geospatial analysis and spatial statistics techniques are powerful tools for mineral prospectivity mapping. These methods incorporate spatial relationships and statistical analyses to identify favorable mineralization environments. Approaches like weights of evidence (Bonham-Carter et al., 1989) and logistic regression (Carranza & Hale, 2001a; Nykänen et al., 2008b) have demonstrated their effectiveness in delineating areas with high mineral potential and assisting in decision-making processes related to exploration targeting.

Recent advancements in geophysical and remote sensing technologies have provided valuable data for mineral prospectivity mapping. Remote sensing techniques, including hyperspectral imaging

and multispectral analysis, can detect mineral signatures, alteration zones and surface expressions of mineral deposits (Wang et al., 2017). Additionally, geophysical methods like airborne and ground-based surveys offer insights into subsurface structures and aid in the identification of potential mineral resources (Airo, 2007).

Three-dimensional (3D) geological modeling and visualization techniques have become indispensable tools for mineral prospectivity mapping. These methods integrate geological, geophysical and geochemical data into a unified 3D framework, enabling detailed visualization and interpretation of the subsurface. By providing a realistic representation of the geological architecture, 3D models facilitate the identification of prospective mineralization zones and guide exploration efforts (Li et al., 2015; Zhang et al., 2020).

The state-of-the-art methods for mineral prospectivity mapping leverage advanced technologies, data integration, machine learning, geospatial analysis, and visualization techniques. These approaches offer improved accuracy, efficiency, and exploration targeting capabilities. However, challenges remain, such as the need for high-quality data, addressing biases in training datasets and improving the interpretability of AI-driven models.

Continued research and development in these areas will further enhance the effectiveness of mineral prospectivity mapping and contribute to sustainable mineral resource exploration (Yousefi et al., 2021).

Selection of Mineral Prospectivity Mapping Method

Based on Bonham-Carter (1994), mineral prospectivity mapping methodologies have two dominant end members: empirical modeling methods (data-driven approach) and conceptual modeling methods (knowledge-driven approach). The first category includes procedures that require known mineral deposits that are used as prior knowledge to train the models (e.g., Bonham-Carter et al., 1989; Bonham-Carter, 1994; Pan & Harris, 2000; Carranza & Hale, 2001a; Mihalasky & Bonham-Carter, 2001; Carranza & Hale, 2002; Harris et al., 2003; Porwal et al. 2003a, 2003b; Carranza et al., 2005; Carranza, 2008; Nykänen, 2008; Nykänen et al., 2008b; Carranza, 2009; Porwal et al., 2010; Zuo & Carranza, 2011; Abedi & Norouzi, 2012; Harris & Grunsky, 2015; Carranza & Laborde, 2016; Zuo & Wang, 2020). Empirical models are especially suitable for areas with large amounts of data, such as brownfield exploration terrains, that have many previously recognized mineral occurrences or deposits to be used for training the models and gaining information about the mineral systems (Yousefi et al., 2021). The second category includes methods that are based on expert subjective judgment on the importance of each evidence data layer describing the critical parameters of the mineral system in question (e.g., Bonham-Carter, 1994; Carranza & Hale, 2001b; Porwal et al., 2003c; Carranza, 2008; Nykänen et al., 2008a; González-Álvarez et al., 2010; Lusty et al., 2012; Lisitsin et al., 2013; Lindsay et al., 2016; Nykänen et al., 2017; Elyasi et al., 2019). It has also been noticed that hybrid models are more commonly used than purely empirical or purely conceptual models (Porwal et al., 2004, 2006; Hronsky & Groves, 2008; Nykänen et al., 2008b).

As previously noted by Nykänen et al. (2008a), the fuzzy logic overlay method is a useful method to translate and simulate expert knowledge for numerical assessment in a GIS platform using a step-by-step practice, as we describe later in Figures 8, 9, 10, 11, 12 and 13 and Tables 2, 3, 4 and 5. Therefore, this technique was selected for the present study.

Mineral Prospectivity Mapping Workflow

Figure 1 describes the main steps of the mineral prospectivity mapping workflow used in this study and by the Geological Survey of Finland in general. It is roughly based on Pan and Harris (2000), Harris and Sanborn-Barrie (2006), Nykänen et al. (2008a) and Knox-Robinson and Wyborn (1997). In this study, we applied fuzzy logic overlay tools in the ArcGIS platform for data integration and in-house-built Python code (Nykänen et al., 2017) for ROC validation. The mineral prospectivity mapping workflow includes the following steps:

1. Development of a mineral systems model for the deposit type in question, and definition of the theoretical criteria for ore formation and related geological processes;
2. Selection of primary data based on the theoretical background and definition of the critical parameters of the mineral systems model;
3. Creation of proxies for the mappable critical parameters, i.e., preprocessing of the primary data into meaningful map patterns. This phase includes rescaling of the data to a common scale from 0 to 1 in fuzzy logic modeling and the application of fuzzy membership functions;
4. Data integration using appropriate methods. In the current study, we chose to use a combination of fuzzy operators (Table 1); and
5. Model validation using known deposits not directly applied in the analysis. In the current study, we used ROC validation and success rate curves.

Fuzzy Logic Overlay

The fuzzy logic overlay method is an adaptable mineral prospectivity mapping method that simulates the decision-making procedure of an exploration team. Consequently, the method is appropriate for testing wide-scale mineral systems model-based prospectivity models, as in the present study. A similar approach has recently also been used, for example, for the IOCG deposit type by Skirrow et al. (2019). The fuzzy logic overlay method that we applied was derived from fuzzy-set theory (Zadeh, 1965), and the method used in this study has previously been described by Nykänen

Table 1. Fuzzy operators (An et al., 1991; Bonham-Carter, (1994; Carranza & Hale 2001b)

Operator	Equation ^a	Description
Fuzzy AND	$\mu_{\text{combination}} = \text{Min}(\mu_A, \mu_B, \mu_C \delta)$	Min. operator, equivalent to Boolean AND (logical intersection)
Fuzzy OR	$\mu_{\text{combination}} = \text{Max}(\mu_A, \mu_B, \mu_C \delta)$	Max. operator, equivalent to Boolean OR (logical union)
Fuzzy algebraic product	$\mu_{\text{combination}} = \prod_{i=1}^n \mu_i$	The output results are always smaller than or equal to the smallest contributing fuzzy membership value
Fuzzy algebraic sum	$\mu_{\text{combination}} = \prod_{i=1}^n (1 - \mu_i)$	The output results are always larger than or equal to the largest contributing fuzzy membership value.
Fuzzy Gamma (γ)	$\mu_{\text{combination}} = \left(\prod_{i=1}^n \mu_i \right)^{1-\gamma} (1 - \prod_{i=1}^n (1 - \mu_i))^\gamma$	This is a combination of the fuzzy algebraic product and the fuzzy algebraic sum.

^a μ_A defines a grade of membership for a map A at a given location, μ_B is the fuzzy membership value for map B, and so on, and μ_i defines the fuzzy membership values for the i th ($i = 1, 2, \dots, n$) maps to be combined.

et al. (2015, 2017). The parameters used in this study are listed in Tables 1, 2, 3 and 4.

The fuzzy operators used to combine various data layers to form the final mineral prospectivity map were “fuzzy AND,” “fuzzy OR” and “fuzzy gamma” (Table 1). The first of these is a minimum operator that yields the minimum cell value of each evidence layer at each location. The second is a maximum operator that yields the maximum cell value, respectively. “Fuzzy gamma” is a combined operator of “fuzzy algebraic sum” and “fuzzy algebraic product.” These “fuzzy operators” have previously been well explained by An et al. (1991), Bonham-Carter (1994) and Carranza and Hale (2001b).

To conduct these GIS operations, we used the ArcGISTM (Esri Inc.) platform with the Spatial AnalystTM extension and the SDM5 toolbox (Geological Survey of Finland, 2022b).

ROC Validation

The “receiver operating characteristics” (ROC) technique (Obuchowski, 2003; Fawcett, 2006; Nykänen et al., 2017) was used to statistically validate the final prospectivity models and intermediate modeling results.

A binary classifier determines whether the value evaluated by some test belongs to a positive or negative group based on a threshold value. Binary classifiers do not always work perfectly, because the distributions of test values sampled by the positive and negative groups overlap for real-life problems. Therefore, some cases will be classified correctly and others will be classified incorrectly. The names of these classes are the following:

1. True negative (TN) (the classifier indicates a negative group, and the real group is negative);
2. False negative (FN) (the classifier indicates a negative group, but the real group is positive);
3. False positive (FP) (the classifier indicates a positive group, but the real group is negative); and
4. True positive (TP) (the classifier indicates a positive group, and the real group is positive).

The ROC validation method used in this study is described by Nykänen et al. (2015, 2017). This method is a graphic validation technique for assessing the performance of binary classifiers. An ROC curve graph displays in a graphical plot the “true positive rate” (“sensitivity”) on the vertical axis and “false positive rate” (“1-specificity”) on the horizontal axis. A critical metric that we use in ROC validation is the area under an ROC curve (AUC), which we use to assess the accuracy of a problem-solving experiment. The AUC rate evaluates the predictive performance of a spatial prognostic model, and it ranges from 0 to 1. A perfectly correct validation result would give an AUC rate of 1, with a “sensitivity” rate of 1 and a “1-specificity” rate of 0. When the predictive model is totally random, the AUC rate would be 0.5 and the curve in the ROC graph would follow the chance diagonal. We used an open-source code for ROC validation (Geological Survey of Finland, 2022b).

To test the results using the ROC method, it is required to have two sets of test data covering the region under exploration containing both true negative and true positive sets. The choice of true negative sets is difficult for spatial prospectivity models of this type, except if confirmed sites are available where it can be guaranteed that no target, i.e., mineral occurrence or deposit, is located within the area. We tested two dis-

Table 2. Summary of the proxies to the critical parameters of the mineral system.

Mineral system component	Theoretical criteria	Mappable criteria	Dataset	Model
Direct detection	Dispersal	Sulfidic rocks	Till geochemistry	All
Direct detection	Conductors	Apparent resistivity	Airborne EM	All
Pathways	Crustal architecture	Proximity to gravity worms	Gravity	All
Pathways	Deep architecture	Proximity to major boundaries	Bedrock map	Magmatic
Pathways	Crustal architecture	Proximity to thrusts	Bedrock map	Ophiolite
Sources	Mantle sources	Mafic to ultramafic rocks	Till geochemistry	Magmatic
Sources	Mantle sources	Proximity to mafic-ultramafic intrusions	Bedrock map	Magmatic
Sources	Mantle sources	Proximity to komatiites	Bedrock map	Magmatic
Sources	Mantle sources	Proximity to layered intrusions	Bedrock map	Magmatic
Sources	Mantle sources	Proximity to volcanic rocks and serpentinites	Bedrock map	Ophiolite
Traps	Favorable host rock	Magnetic field total intensity	Airborne magnetics	All
Traps	Radiometric anomaly	Uranium radiation anomaly	Airborne Gamma radiation	Black shale, Kuusamo
Traps	Favorable host rock	Proximity to black shales	Bedrock map	Black shale
Traps	Favorable host rock	Permissive tracts (favorable lithology)	Bedrock map	Kuusamo
Traps	Favorable host rock	Proximity to albite rocks	Bedrock map	Kuusamo

Model names: magmatic = orthomagmatic deposits, ophiolites = ophiolite-related deposits, black shale = black shale-related deposits, Kuusamo = Kuusamo-type deposits

similar “*negative*” sets: (1) arbitrary positions as true negative sets, as, for example, in Nykänen et al. (2017) and (2) selected industrial mineral deposits plus lithium pegmatites taken from the mineral deposit database (Geological Survey of Finland, 2016). Another possibility would be to use drilling data with barren drillholes that have not intersected relevant mineralization as negative training sites, but we envision that these would also introduce a bias due to selection of the target area for drilling in many cases. Therefore, we consider the usage of other, non-sulfidic deposit types as a robust method for selecting true negative sites for validation. True positive sets were characterized by previously identified Co-bearing mineral occurrences and drilling sites. Graphs and AUC values derived from both options for true negative sets are presented in Figures 8, 9, 10, 11, 12 and 13 for comparison.

Success Rate Curves

Success rate curves showing the efficiency of prediction were defined by comparing the modeling results (i.e., the mineral prospectivity map) and the known mineral deposits or drilling sites exceeding a

certain assay threshold. We followed the methods previously used, for example, by Chung and Fabbri (2003), Harris et al. (2001) and Harris et al. (2015). We plotted the cumulative percentage area ordered from high to low prospectivity values on the *x*-axis and the cumulative number of Au sites captured in this area on the *y*-axis. In our case, the validation sites were known mineral deposits (Geological Survey of Finland, 2016) for the four different deposit models and drilling sites with assayed samples containing over 500 ppm Co for the combined model. From the 1266 qualified drilling sites, we selected drilling sites more than 1 km apart from each other, ending up with 221 validation points within the study area. From these graphs, one can observe how large a predictive area is needed to capture the Co-bearing drilling sites. The smaller the area containing more drilling sites, the more efficient the model is. Another way to verify model efficiency is to derive the area under this success rate curve. This value relates to model efficiency in correctly classifying training points, with higher AUC values indicating better performance. The success rate curves for this study are plotted together with the ROC curves in Figures 8, 9, 10, 11, 12 and 13, showing the prospectivity models.

Table 3. Orthomagmatic fuzzy model

Layer no.	Input layer name	Fuzzy membership function/operator parameters	ROC AUC
1	Till Ti	Large, MP = 1298, $S = 2$	
2	Till Cr	Large, MP = 28, $S = 1$	
3	Till Mg	Large, MP = 4933, $S = 2$	
4	Till Ni	Large, MP = 20, $S = 1$	
5	Till Co	Large, MP = 9, $S = 2$	
6	Till Cu	Large, MP = 26, $S = 2$	
7	Magnetics	Large, MP = 7000, $S = 8$	
8	Apparent resistivity	Small, MP = 1752, $S = 5$	
9	Proximity to gravity worms	Small, MP = 3000, $S = 1$	
10	Proximity to mafic-ultramafic intrusions	Small, MP = 10000, $S = 1$	
11	Proximity to komatiites	Small, MP = 10000, $S = 1$	
12	Proximity to layered intrusions (2400 Ma)	Small, MP = 10000, $S = 1$	
13	Proximity to gravity worms over 10 km depth	Small, MP = 20000, $S = 5$	
14	Proximity to major boundaries	Small, MP = 50000, $S = 1$	
	<i>Intermediate fuzzy overlays</i>		
15	Till Rocks Gamma	Gamma = 0.55 (layers 1, 2 and 3)	0.598
16	Till Sulf Gamma	Gamma = 0.55 (layers 4, 5 and 6)	0.645
17	Geochem AND	AND (layers 15 and 16)	0.632
18	Geophysics Gamma	Gamma = 0.6 (layers 7, 8 and 9)	0.6
19	Geol OR	OR (layers 10, 11 and 12)	0.91
20	Gamma major boundaries/worms	Gamma = 0.65 (layers 13 and 14)	0.626
21	Geol AND	AND (layers 19 and 20)	0.797
	<i>Final prospectivity map</i>		
22	Orthomagmatic Co Gamma	Gamma = 0.75 (17, 18 and 21)	0.773

Number of validation sites = 210

MP midpoint, S spread

Table 4. Ophiolite-related fuzzy model

Layer no.	Input layer name	Fuzzy membership function/operator parameters	ROC AUC
1	Till Ti	Large, MP = 1298, $S = 2$	
2	Till Cr	Large, MP = 28, $S = 1$	
3	Till Mg	Large, MP = 4933, $S = 2$	
4	Till Ni	Large, MP = 20, $S = 1$	
5	Till Co	Large, MP = 9, $S = 2$	
6	Till Cu	Large, MP = 26, $S = 2$	
7	Till Zn	Large, MP = 32, $S = 2$	
8	Magnetics	Large, MP = 7000, $S = 8$	
9	Apparent resistivity	Small, MP = 737, $S = 2$	
10	Proximity to gravity worms	Small, MP = 3000, $S = 1$	
11	Proximity to thrusts	Small, MP = 10000, $S = 1$	
12	Proximity to volcanic rocks and serpentinites	Small, MP = 10000, $S = 1$	
	<i>Intermediate fuzzy overlays</i>		
16	Till Rocks Gamma	Gamma = 0.75 (layers 1, 2 and 3)	0.741
17	Till Sulf Gamma	Gamma = 0.75 (layers 4, 5, 6 and 7)	0.861
18	Geochem AND	AND (layers 16 and 17)	0.831
19	Geophysics Gamma	Gamma = 0.6 (layers 8, 9 and 10)	0.832
20	AND ophiolites	AND (11 and 12)	0.971
	<i>Final prospectivity map</i>		
23	OKU type Gamma	Gamma = 0.5 (18, 19 and 20)	0.99

Number of validation sites = 10.

MP midpoint, S spread

STUDY AREA

Fennoscandian Shield

This study was conducted within the north-westernmost part of the East European Craton, and more specifically within the northern Fennoscandian Shield (Fig. 2). The Archaean basement within this area is split into three cratonic centers: the Norrbotten, Karelian and Kola cratons. These cratonic areas were possibly created separately from each other, were fragmented into pieces from 2.51 to 2.4 Ga, and finally merged together roughly 1.9 Ga ago (Lahtinen et al., 2014). Between 1.9 and 1.8 Ga, several juvenile volcanic arcs and microcontinents were accreted predominantly on the southwest boundary of the Archaean craton. This finally formed the present-day Fennoscandian Shield by carbonization by 1.77 Ga (Lahtinen et al., 2014). Neoproterozoic and Phanerozoic cover sequences overlie and unconformably bound the Fennoscandian Shield to the east and south. The Early Paleozoic Caledonian orogen bounds the Fennoscandian Shield to the north and west.

Co-Enriched Mineral Systems in Finland

Based on work by Mudd et al. (2013), three deposit categories cover the majority (roughly 85%) of world-wide cobalt resources, and these mineral deposit types include magmatic Ni–Cu–Co (+PGE), Ni–Co laterite deposits and stratiform sediment-hosted deposits. It is quite often possible that there are local variations in terms of the deposit types that are dominant, and in Finland, for example, four main cobalt-bearing deposit types are recognized (Horn et al., 2021): (1) orthomagmatic sulfide deposits, (2) ophiolite-related VMS deposits (Outokumpu type), (3) black shale-related deposits (Talvivaara type) and (4) supracrustal rock-hosted deposits (Kuusamo type). All of these are drilling indicated, and we used the mineral deposit database (Geological Survey of Finland, 2016) for model validation and model performance assessment. Various deposit types are described in detail below.

Orthomagmatic Sulfide Ore Deposits

According to Horn et al. (2021), magmatic sulfide ore deposits are globally the most important

source of nickel and copper, with cobalt being a by-product of these types of ore deposits. Deposits in this category are associated with upper mantle-derived mafic to ultramafic rocks (Eckstrand & Hulbert, 2007; Naldrett, 2011). The formation of sulfide ore bodies is possible when nickel, copper and cobalt are separated in an immiscible sulfide melt, when the magma turns out to be saturated with sulfur, normally because of contact with crustal rocks (e.g., Naldrett, 2011). Under perfect physical conditions, these may form an economic deposit. Pyrrhotite, pentlandite and chalcopyrite are the dominant ore minerals in these ore deposits, but pentlandite mainly hosts cobalt in these ores (Schulz et al., 2014; Barnes et al., 2018). According to Naldrett (2004), the globally most significant deposits are in the Norilsk-Talnakh area of Russia, in Voisey's Bay in Labrador, Canada, and in the Sudbury area of Ontario, Canada. Norilsk-Talnakh deposits occur in chonolith- to sill-type intrusions produced by rifting-related magmatism forming the Siberian traps, as described by Eckstrand and Hulbert (2007), while deposits of the Voisey's Bay type are accommodated in high-Al basaltic rock types based on Scoates and Mitchell (2000). According to Eckstrand and Hulbert (2007), the Sudbury area can be considered as exceptional, as within this region, magmatic sulfide deposits are associated with magma that resulted from a huge meteorite impact, and it is not therefore easily comparable with other areas. There are also examples of cobalt-bearing nickel ores that are associated with komatiitic lava flows and sills, such as Kambalda in Australia and Raglan in Canada (Eckstrand and Hulbert, 2007; Naldrett, 2011). Within our study area, there are 210 deposits in this orthomagmatic category (Figs. 3 and 8) when combining three different deposit types, so this is the most widespread and dominant deposit type in this study. These deposits were combined from the following deposit types: (1) deposits related to Svecofennian (1.9–1.75 Ga age) and other (Archaean to Paleoproterozoic) mafic to ultramafic intrusions (Weihed et al., 2005; Makkonen, 2015), (2) deposits related to mafic-ultramafic layered intrusions of 2.44 Ga age (Lahtinen et al., 2011) and (3) deposits related to komatiitic rocks of 3.5–2.06 Ga age (Konnunaho et al., 2015; Makkonen et al., 2017).

Ophiolite-Related Deposits (Outokumpu Type)

Outokumpu-type mineral deposits are currently limited to the region of Outokumpu in the North

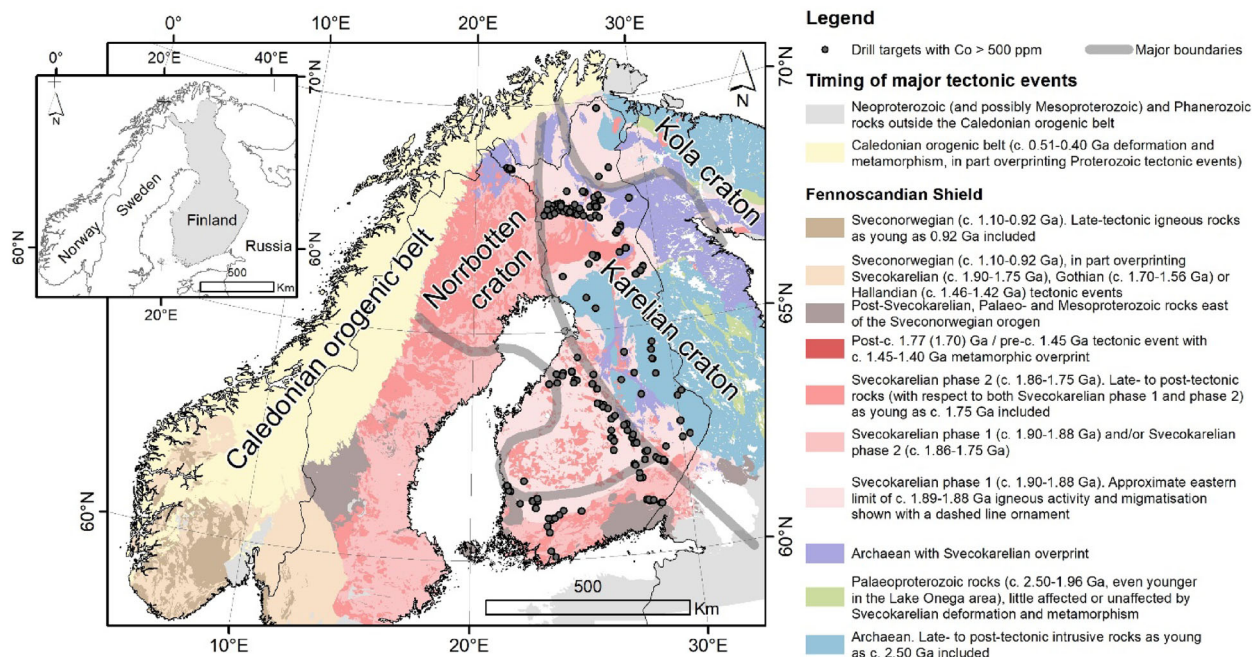


Figure 2. Location of the study area. Drilling targets represent exploration drilling with Co > 500 ppm. The generalized geological map is modified from Koistinen et al. (2001). Major tectonic boundaries, including the approximate craton boundary and micro-continent boundaries, from Lahtinen et al. (2014) and Lahtinen and Huhma (2019).

Karelian Schist Belt in eastern Finland and represent volcanogenic massive sulfide deposit (VMS) type. We classified the 10 deposits (Figs. 3 and 9) occurring in this area as “*ophiolite-related deposits*” (Peltonen et al., 2008). They occur as ruler-shaped forms or lenses of massive to semi-massive sulfides, of which the Outokumpu deposit was the most significant, with 28 Mt containing 3.8% Cu, 1.1% Zn, 0.24% Co and 0.12% Ni (Parkkinen, 1997). Cobalt and nickel enriched VMS deposits are relatively rare, the closest analogue being southern Urals VMS deposits, some of which also contain both Co and Ni e.g., Ishkinino and Ivanovka (Nimis et al., 2008).

Peltonen et al. (2008) proposed a two-phase formation model for the polymetallic Cu–Co–Zn–Ni–Ag–Au deposits of the Outokumpu ore district: the original ore type of VMS Cu–Zn was formed by hydrothermal sulfide accumulation on the ultramafic-dominant ocean floor during a late rifting event (1.95 Ga) (Peltonen et al., 2008). During later events, the ultramafic seafloor together with the sulfide-bearing ore bodies were obducted along the edges of the Karelian Craton, forming the Outokumpu Allochthon (Peltonen et al., 2008). At the same time, the Cu–Co–Zn–Ni–Ag–Au deposits were formed through syntectonic mixing of the Cu proto-ore and disseminated Ni(–Co) sulfides in quartz–

carbonate rocks (highly altered mantle peridotites) by fluid-assisted mobilization of the proto-ore into the quartz–carbonate rocks. Alternatively, the unusual Co and Ni enrichment could be a primary feature of the hydrothermal system, related to fluid temperature and chemistry and the ultramafic nature of the paleo sea floor. In these deposit types, cobalt is mainly hosted by pyrite and cobalt pentlandite, and in more arsenic-rich parts, but less frequently, the host can be cobaltite (e.g., Peltola, 1978; Reino, 1980; Huhtelin and Sotka, 1994; Peltonen et al., 2008)

Black Shale-Related Deposits (Talvivaara Type)

In eastern Finland, there are 25 black shale-hosted deposits and occurrences associated with the Paleoproterozoic Kainuu Schist Belt, which is located adjacent to the Archaean-Proterozoic border (Figs. 3 and 10). These occurrences incorporate the Sotkamo deposit (1458 Mt with 0.25% Ni, 0.52% Zn, 0.14% Cu and 0.019% Co), currently producing nickel, copper, zinc and cobalt and also being the main cobalt source in Europe, with a known resource of ~ 300,000 tons of contained cobalt (Terrafame, 2021). Organic-rich mud and sand were

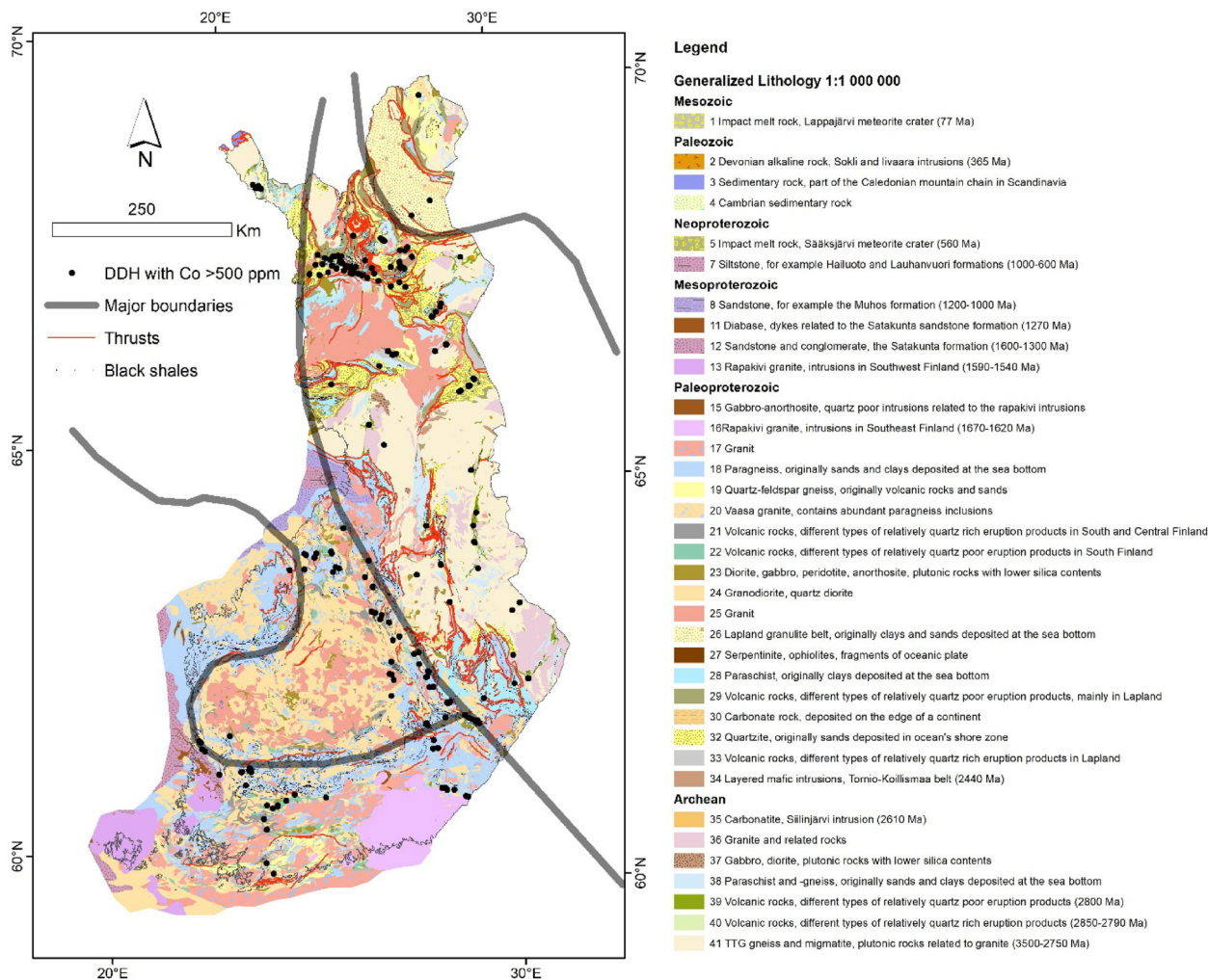


Figure 3. Generalized geological map of the study area at scale 1:1,000,000 (Bedrock of Finland - DigiKP, 2018). Drilling targets with Co > 500 ppm were used as validation sites for the combined prospectivity model. Major tectonic boundaries, including the approximate craton boundary and micro-continent boundaries, from Lahtinen et al. (2014) and Lahtinen and Huhma (2019), are the same as in Fig. 1. Thrusts and black shales are from Bedrock of Finland—DigiKP (2018).

deposited in a stratified, anoxic-euxinic marine basin between 2.1 and 1.9 Ga, forming carbon- and sulfur-rich black shales, which host the deposits (Loukola-Ruskeeniemi and Lahtinen, 2013; Kontinen and Hanski, 2015). The current thick succession (up to 300 m) of highly metalliferous black shales is thought to be a combination of resedimentation processes such as turbidity currents and tectonic repetition due to the Svecofennian orogeny (ca. 1.91–1.78 Ga), which also resulted in variable sulfide mobilization and grain coarsening (Loukola-Ruskeeniemi & Lahtinen, 2013; Kontinen & Hanski, 2015).

Supracrustal Rock-Hosted Deposits (Kuusamo Type)

There are several cobalt-bearing epigenetic deposits in volcano-sedimentary belts of northern Finland (Central Lapland Greenstone Belt, the Peräpohja Belt and the Kuusamo Belt), where these deposits are related to supracrustal sequences dominated by mafic to ultramafic volcanic rocks, quartzites, meta-arkoses and mica schists, which were deformed during the Svecofennian orogeny. Cobalt is related to gold and copper in these deposits, occurring as discrete cobalt minerals (cobaltite, Co-pentlandite, and also as linnaeite at

Rajapalot), as well as minor constituents in pyrite and pyrrhotite (Vanhanen, 2001; Eilu, 2015; Molnár et al., 2017a; Pohjolainen et al., 2017; Köykkä et al., 2019; Raic et al., 2022). The deposits display features typical of orogenic Au deposits with an atypical metal association (Groves et al., 1998; Groves et al., 2018) and share similarities with Co-enriched gold deposits in the Idaho Cobalt Belt (Slack et al., 2010). The deposits occur within a particular stratigraphic level within the Paleoproterozoic sequence (Vanhanen, 2001; Molnár et al., 2016; Vasilopoulos et al., 2021). The enrichment of Co and Cu in the deposits is suggested to be related to elevated salinities in the mineralizing fluids, the source for the chlorine being evaporites within the ore-hosting sequence (Ranta et al., 2020; Tapio et al., 2021; Vasilopoulos et al., 2021). All these areas are under active exploration, e.g., the Juomasuo and Sivakkaharju deposits in Kuusamo (Latitude 66 Cobalt, 2019) and the Rajapalot Au–Co development in the Peräpohja Belt (Ranta et al., 2018). The number of known deposits of this type in the mineral deposit database is 23 (Figs. 3 and 11).

PRIMARY DATA USED TO DEFINE PROXIES FOR CRITICAL PARAMETERS OF THE MINERAL SYSTEM MODELS

Geological Map

The bedrock map used in this study was derived from the Bedrock of Finland 1:200,000 (Bedrock of Finland - DigiKP, 2018), which can be described as a unified bedrock map of Finland. It has been compiled over the years by generalizing the scale-free bedrock map feature dataset to the scale 1:200,000. The data have not been generalized within those parts where the source data are at a poorer scale than 1:200,000. Furthermore, this digital map dataset is composed of lithological and stratigraphical geological polygon and linear layers, representing faults, various other structural lines and dykes (Fig. 3). The stratigraphic geological unit polygon map layer consists of lithological coding, the geological time period and hierarchical lithostratigraphic or lithodemic classification as attributes. The line layers have their own hierarchical classification. The faults have been classified based on the size and type of the

faults. The dataset also has adequate metadata, following ISO 19115:2005 standard.

Geophysics

Finland has total coverage of a high-resolution aerogeophysical survey data, including concurrent magnetic, radiometric and electromagnetic surveys (Airo, 2005). These surveys were typically flown at 40 m altitude and 200 m line spacing, and the flight direction varied between flight areas depending on the local geology. The usage of these surveys in the mineral prospectivity mapping is described by Nykänen et al. (2017). We interpolated the airborne geophysical line data with a 50 × 50 m grid cell size using the minimum curvature interpolation technique and re-sampled to a 100 × 100 grid cell size so that we had an equal cell size to all the other input data.

A Bouguer anomaly map at 1:2M scale covering the entire Fennoscandian Shield, compiled by Korhonen et al. (2002), was used in this study, as it is the only available gravity dataset covering the entire study area. For the mineral prospectivity analysis, we performed proximity analysis for the detected gravity gradient maxima zones or worms, as fault-related gradients can be relevant to mineral deposits (Murphy, 2010). The resulting grids had a cell size of 100 × 100 m. The geophysical maps used in the modeling are presented in Figure 4.

Geochemistry

A county-wide till geochemical sampling program was organized in Finland from 1982 to 1994 (Salminen, 1995) and was used in this study, as described in more detail, for example, by Nykänen et al. (2017). For this study, we interpolated grids using the inverse distance weighting (IDW) method with a 100 × 100 m cell size. We used a variable search radius and included 12 samples to perform each interpolation. With this method, we were able to control the number of samples used for interpolation. The elements interpolated are discussed in the results chapter below, where the models are also described. The geochemical maps used in the modeling are presented in Figures 5, 6 and 7.

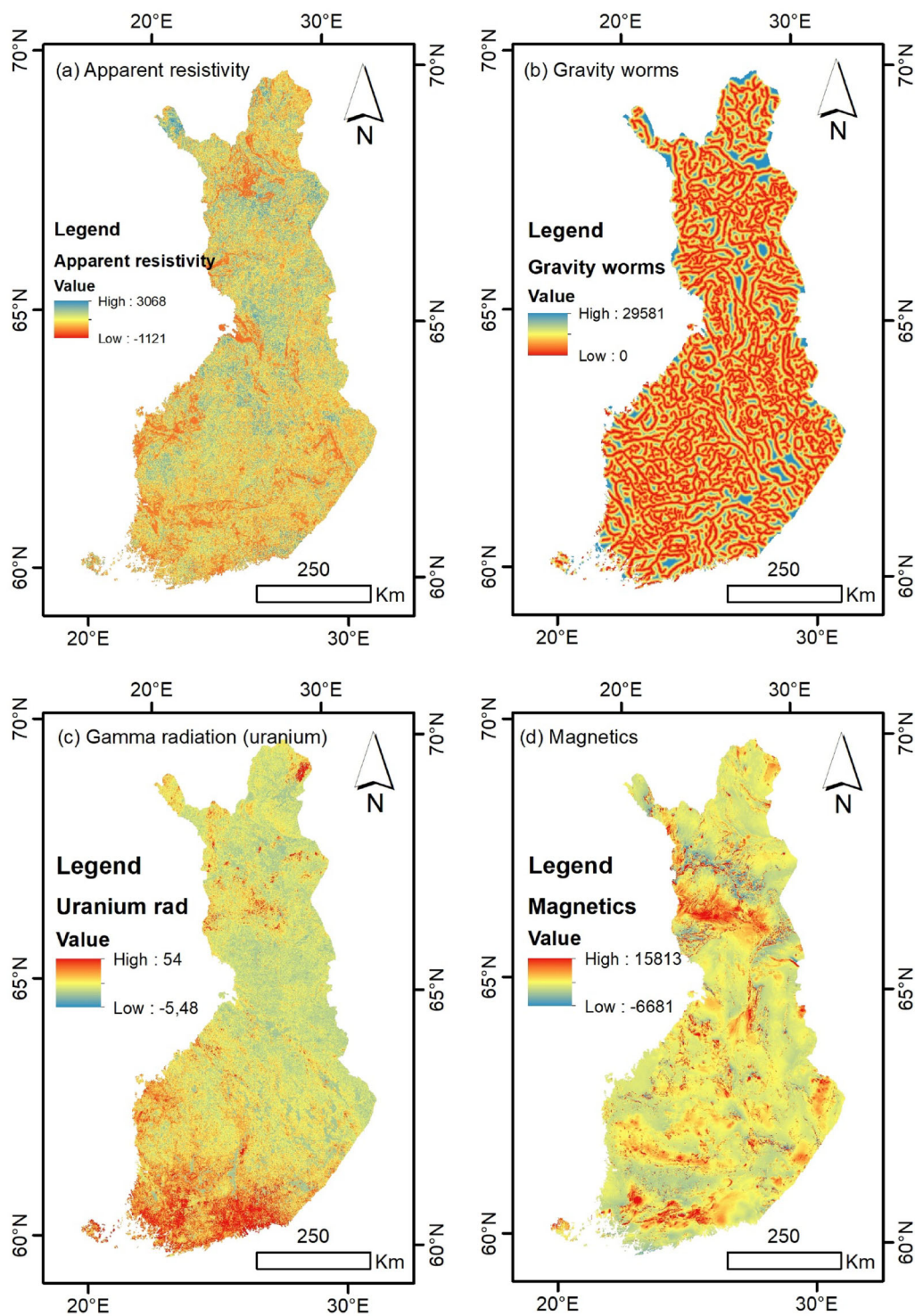


Figure 4. Geophysical data used for mineral prospectivity assessment in this study: (a) apparent resistivity, (b) gravity gradient maxima (worms) calculated from the upward-continued regional Bouguer anomaly maps, (c) airborne gamma radiation (uranium channel) and (d) airborne magnetic field total intensity.

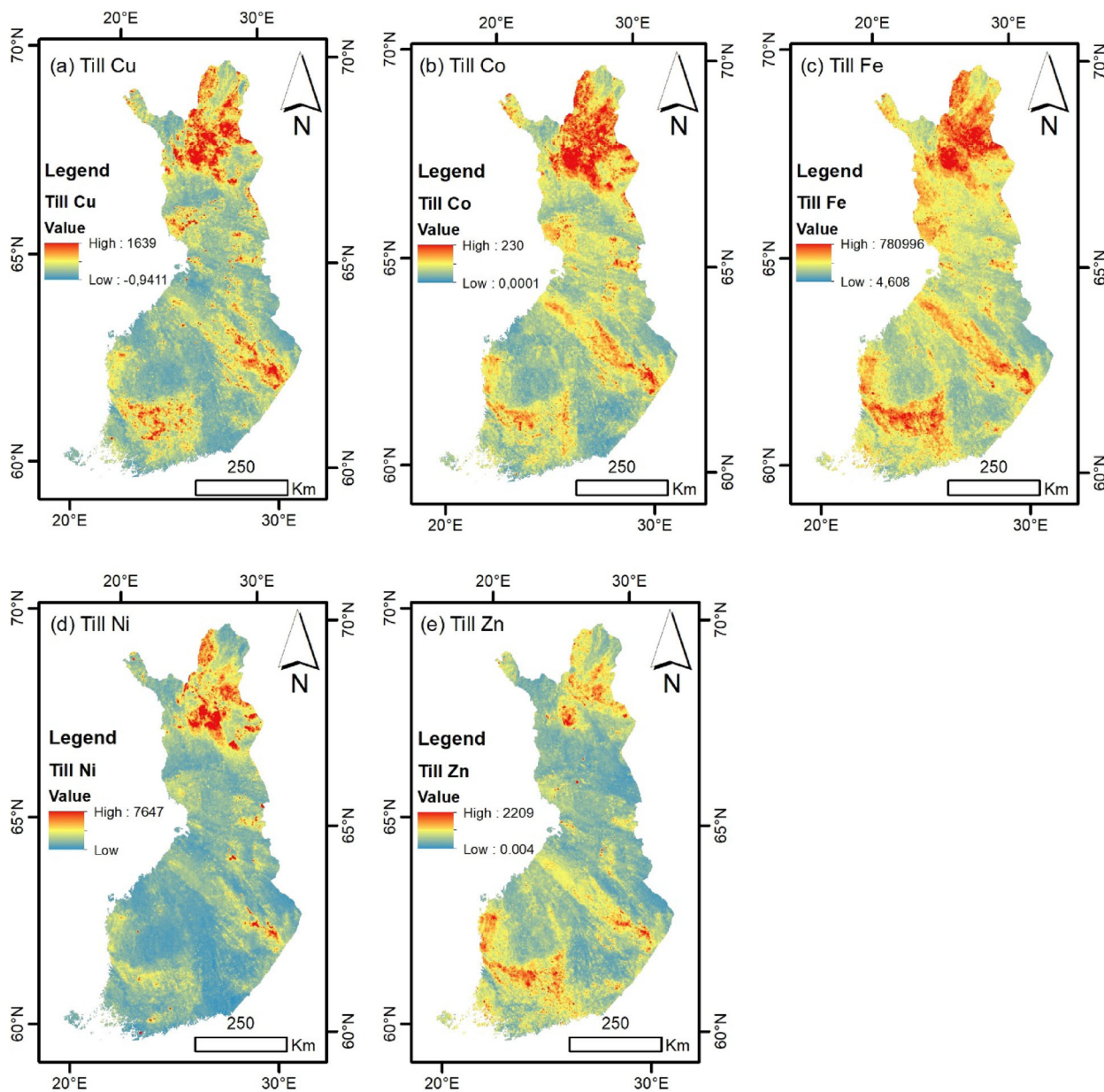


Figure 5. Inverse-distance interpolated till geochemistry grids: (a) Cu, (b) Co, (c) Fe, (d) Ni and (e) Zn.

RESULTS OF COBALT PROSPECTIVITY MAPPING

Orthomagmatic Deposits

The summary of the mineral system components and the fuzzy overlay model describing the orthomagmatic cobalt-bearing deposits are presented in Tables 2 and 3, respectively. From the

geochemical data, we first combined titanium, chromium and magnesium using the “fuzzy gamma” operator to represent mafic to ultramafic lithological rock units and then nickel, cobalt and copper using the “fuzzy gamma” operator to represent sulfides. Then, these were combined into an intermediate geochemical layer using the “fuzzy AND” operator. Following this, we combined airborne magnetic anomalies and low resistivity zones with gravity

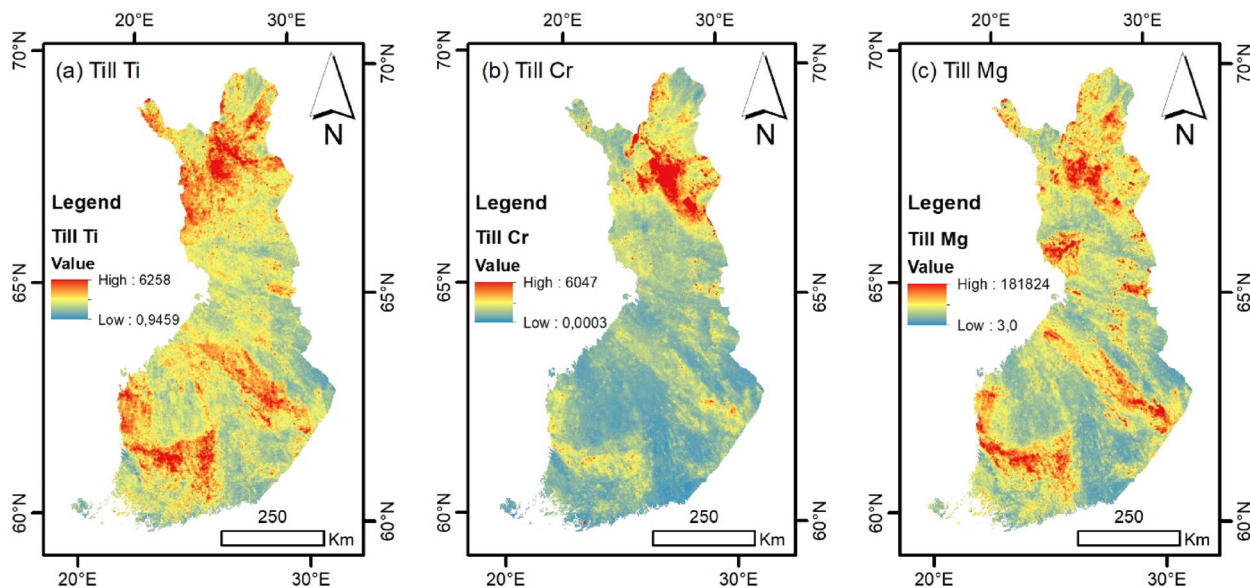


Figure 6. Inverse-distance interpolated till geochemistry grids: (a) Ti, (b) Cr and (c) Mg.

worms using the “fuzzy gamma” operator to create the geophysical response. Finally, the geological layers, namely mafic to ultramafic intrusions, layered intrusions and komatiitic rocks, were integrated using the “fuzzy OR” operator, major boundaries and gravity worms were combined with the “fuzzy gamma” operator, and these two intermediate layers were then combined with the “fuzzy AND” operator to generate a geological response layer. As mentioned earlier, we had 210 deposits within these categories when we combined the three different deposit types. These deposits were used for validation of the intermediate layers and the final prospectivity map (Fig. 8), which was created applying the “fuzzy gamma” operator. The AUC values are moderate and the AUC value of the final prospectivity map is 0.773 when using random negative sites and 0.726 when using true negative sites. The efficiency curve illustrates that within 10% of the area, the model captures 40% of the known deposits. The area under the efficiency curve is 77%.

This model performs relatively well in classifying the known orthomagmatic Ni–Cu occurrences and also indicates new potential exploration areas, especially within the central Lapland area and the Ostrobothnia area within the Hitura region (Fig. 8).

In addition, southern Finland and the Outokumpu region appear to have high prospectivity for this deposit type.

Ophiolite-Related Deposits

The summary of the mineral system components and the fuzzy overlay model describing ophiolite-related cobalt-bearing deposits are presented in Tables 2 and 4, respectively. From the geochemical data, we first combined titanium, chromium and magnesium using the “fuzzy gamma” operator to represent mafic to ultramafic lithological rock units, and then nickel, cobalt and copper using the “fuzzy gamma” operator to represent sulfides. These were then combined into an intermediate geochemical layer using the “fuzzy AND” operator. Airborne magnetic anomalies and low resistivity zones were combined with gravity worms using the “fuzzy gamma” operator to create the intermediate geophysical response. To define the zones with potential for ophiolites, we combined proximity to thrusts and proximity to serpentinites and volcanic rocks with the “fuzzy AND” operator. The final prospectivity map (Fig. 9) was created by using the “fuzzy gam-

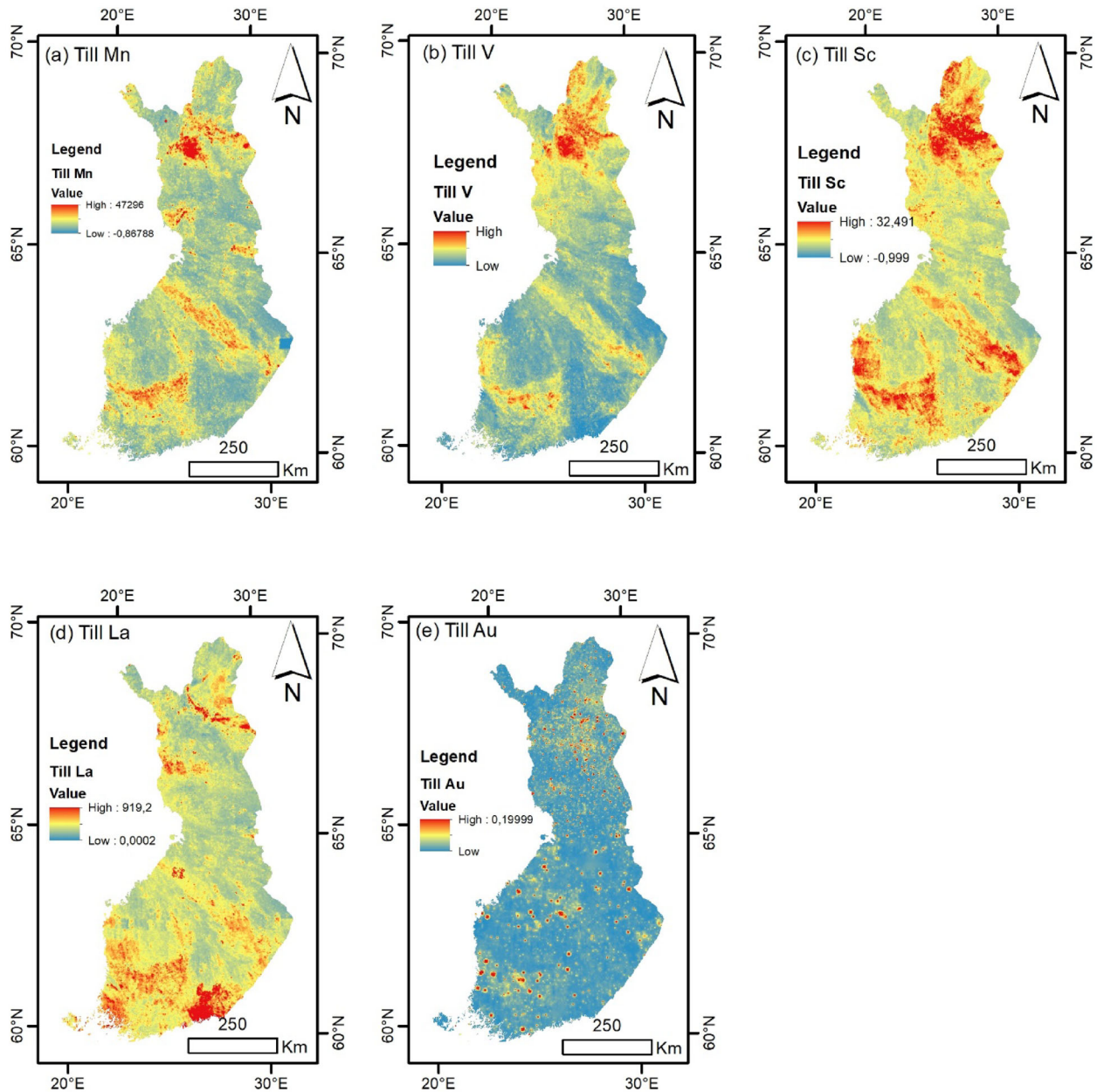


Figure 7. Inverse-distance interpolated till geochemistry grids: (a) Mn, (b) V and (c) Sc, (d) La and (e) Au.

ma'' operator. We only had 10 known deposits belonging to this category, so the relatively high AUC values of 0.99 and 0.945 can be considered very uncertain. The efficiency curve also has a high AUC value (97%), and the model captures 100% of the known deposits within 10% of the area.

The Outokumpu region, where the type deposits are located, is the most favorable area based on the modeling results (Fig. 9), but the central Lapland region also appears to have potential. All other regions are only moderately favorable.

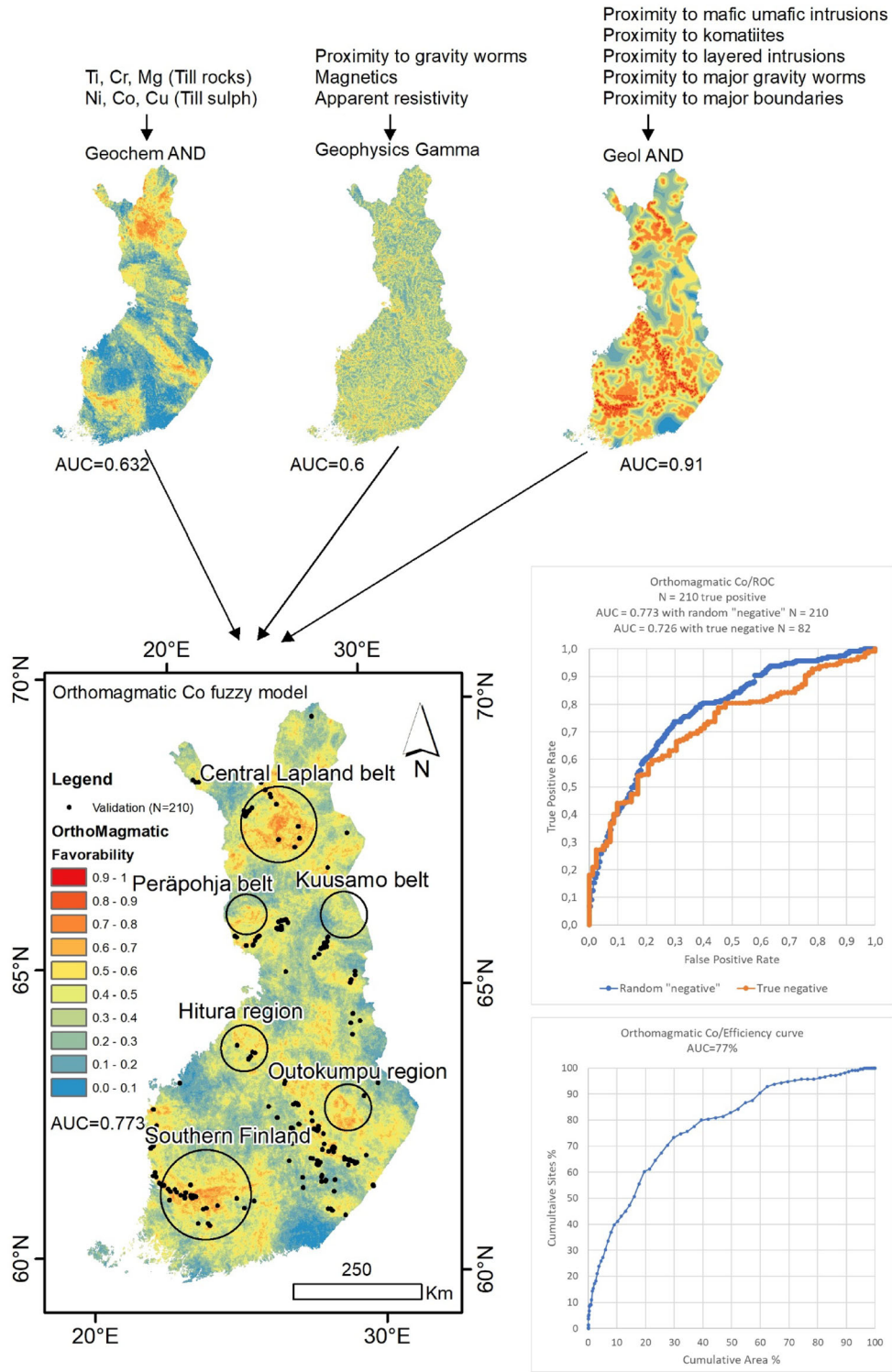


Figure 8. Orthomagmatic Co fuzzy overlay mineral prospectivity model.

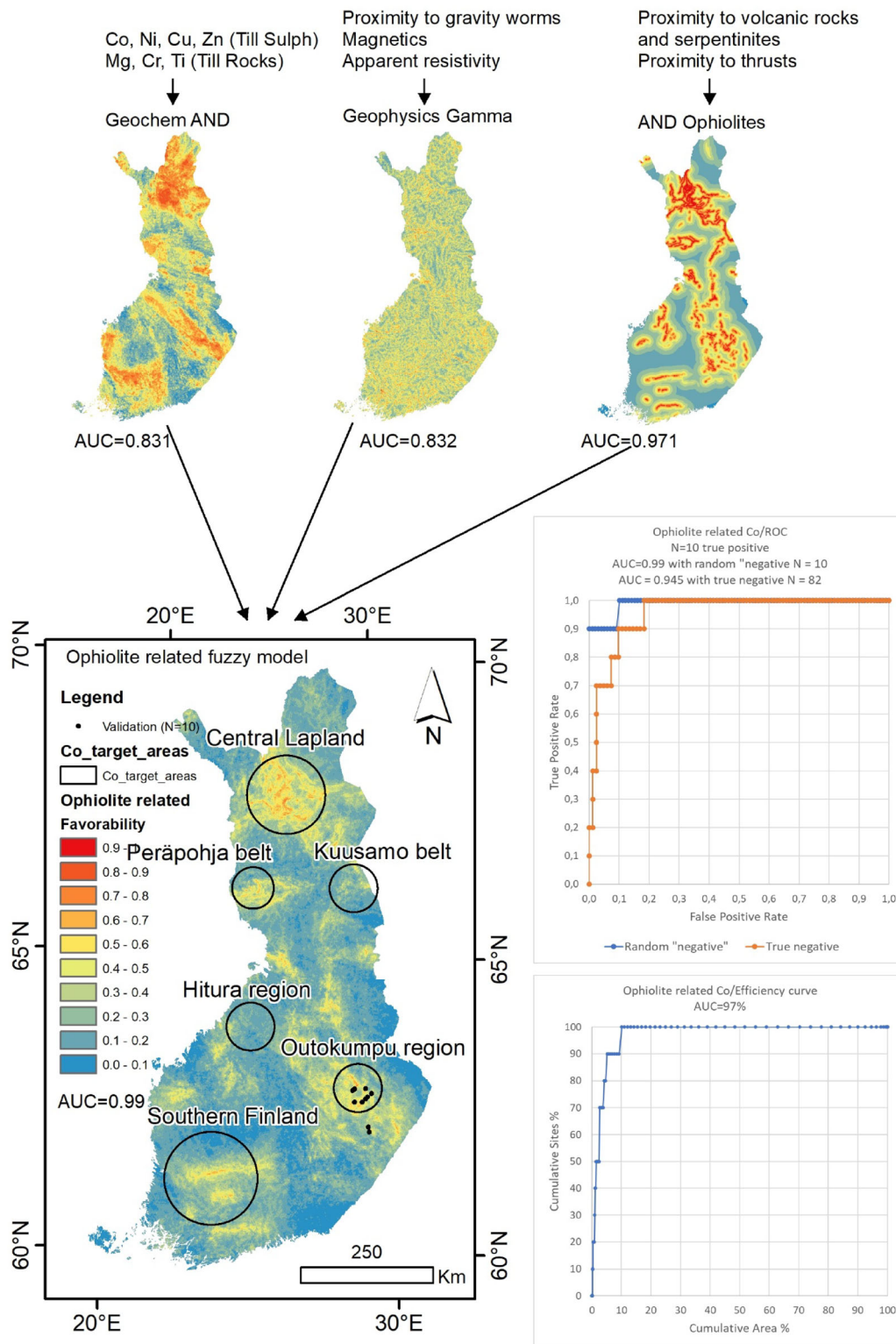


Figure 9. Outokumpu-type fuzzy overlay mineral prospectivity model.

Table 5. Black shale-related fuzzy model

Layer no.	Input layer name	Fuzzy membership function/operator parameters	ROC AUC
1	Till Co	Large, MP = 9, S = 2	
2	Till Ni	Large, MP = 20, S = 1	
3	Till Zn	Large, MP = 32, S = 2	
4	Till Cu	Large, MP = 26, S = 2	
5	Till Mn	Large, MP = 111, S = 2	
6	Till Fe	Large, MP = 18289, S = 2	
7	Till V	Large, MP = 42, S = 2	
8	Till Sc	Large, MP = 4, S = 2	
9	Uranium radiation	Large, MP = 7, S = 8	
10	Magnetics	Large, MP = 7000, S = 8	
11	Apparent resistivity	Small, MP = 1858, S = 2	
12	Proximity to gravity worms	Small, MP = 3000, S = 1	
13	Proximity to black shales	Small, MP = 2500, S = 1	0.989
	<i>Intermediate Fuzzy overlays</i>		
14	Till Sulf Gamma	Gamma = 0.75 (layers 1, 2, 3 and 4)	0.734
15	Till Oxides Gamma	Gamma = 0.75 (layers 4, 5, 6, 7 and 8)	0.559
16	Geochem GAMMA	Gamma = 0.5 (layers 14 and 15)	0.665
17	Geophysics Gamma	Gamma = 0.75 (layers 9, 10, 11 and 12)	0.842
	<i>Final prospectivity map</i>		
18	Black Shale-related Co	Gamma = 0.45 (13, 16 and 17)	0.959

Number of validation sites = 25.

MP midpoint, S spread

Black Shale-Related Deposits

The summary of the mineral system components and the fuzzy overlay model describing cobalt-bearing black shale-related deposits are presented in Tables 2 and 5, respectively. From the geochemical data, we first combined cobalt, nickel, zinc and copper using the “fuzzy gamma” operator to represent sulfides. Then, we combined manganese, iron, vanadium and scandium to represent oxides using the “fuzzy gamma” operator. These two geochemical layers were combined using the “fuzzy gamma” operator. Geophysical data were combined by integrating uranium radiation, magnetics and apparent resistivity using the “fuzzy gamma” operator. The final prospectivity map (Fig. 10) was created by applying the “fuzzy gamma” operator. ROC validation was performed by using 25 known deposits, and the AUC value of 0.959 for the final prospectivity map is relatively high. With true negative sites, the AUC value is clearly lower, being 0.895. The efficiency curve indicates that the model captures 90% of the known deposits within 10% of the area. The AUC value of the efficiency curve for this model is 95%. According to statistical validation, this model performs well in classifying the known black shale-related deposits in the Kainuu region,

but also indicates new potential areas in southern Finland and in the central Lapland area.

Kuusamo-Type Deposits

The summary of the mineral system components and the fuzzy overlay model describing Kuusamo-type cobalt-bearing deposits are presented in Tables 2 and 6, respectively. From geochemistry, we integrated gold, copper, cobalt and lanthanum, applying the “fuzzy gamma” operator. Proximity to gravity worms and permissive lithological units (Rasilainen et al., 2020) were merged using the “fuzzy AND” operator. The final prospectivity map (Fig. 11) was created by integrating all the intermediate layers with the “fuzzy gamma” operator. ROC validation was performed using 23 known deposits, and the AUC value of the final prospectivity map is 0.972 with random negative sites. When using industrial mineral sites as true negative sites, the AUC value is 0.945. Based on the efficiency curve, the model captures 90% of the known deposits within 10% of the area. The AUC value of the efficiency curve is also relatively high, being 97%.

This model performs well in classifying the known deposits within the Kuusamo Belt and

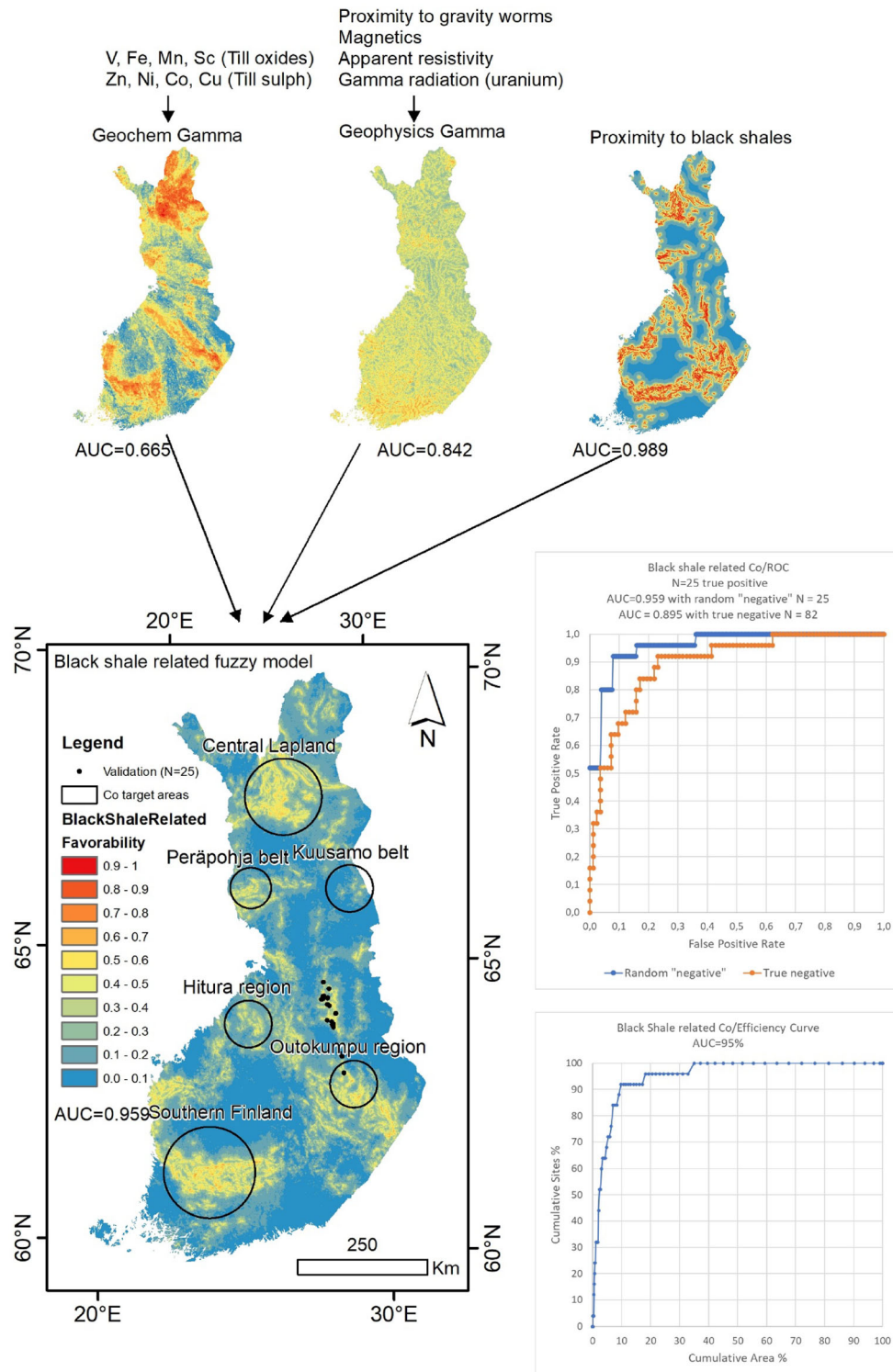


Figure 10. Black shale-related Co fuzzy overlay mineral prospectivity model.

Table 6. Kuusamo type fuzzy model.

Layer no.	Input layer name	Fuzzy membership function/operator parameters	ROC AUC
1	Till Au	Large, MP = 0.002, S = 2	
2	Till Cu	Large, MP = 26, S = 2	
3	Till Co	Large, MP = 9, S = 2	
4	Till La	Large, MP = 25, S = 2	
5	Uranium radiation Median 4 km	Large, MP = 2, S = 3	
6	Apparent resistivity	Small, MP = 1600, S = 5	
7	Magnetic	Large, MP = 6600, S = 5	
8	Proximity to gravity worms	Small, MP = 10000, S = 2	
9	Proximity to favorable lithology (permissive tracts)	Small, MP = 3000, S = 1	
10	Proximity to albite rocks <i>Intermediate Fuzzy overlays</i>	Small, MP = 10000, S = 2	
11	Sulf Gamma	Gamma = 0.5 (2 and 3)	0.508
12	Geochem AND	AND (layers 1, 4 and 11)	0.657
13	Geol AND	AND (layers 8, 9 and 10)	0.982
14	Geoph Gamma <i>Final prospectivity map</i>	Gamma = 0.75 (layers 5, 6 and 7)	0.517
15	Kuusamo Gamma	Gamma = 0.75 (12, 13 and 14)	0.973

Number of validation sites = 29

MP midpoint, S spread

Peräpohja Belt and also predicts potential new areas for this deposit type within the central Lapland area, where some atypical orogenic gold occurrences with enriched cobalt have only rarely been found (e.g., Holma & Keinänen, 2007; Vasilopoulos et al., 2021). Other orogenic gold deposits with an atypical metal association have also been recognized within the central Lapland area (e.g., Molnár, 2019).

Combined Model

The combined model (Fig. 12) integrates all the previous models into a total cobalt endowment map for Finland, delineating all the favorable areas for cobalt exploration. We used the “fuzzy OR” operator, which returns the maximum value of each input layer. This model provides an overview of all the separate models at the same time. For ROC validation, we used 221 drilling sites with assayed samples containing over 500 ppm cobalt as true positive sites and two sets of true negative sites: random sites and sites with industrial minerals. The AUC values of the ROC validations are almost identical for random and industrial mineral sites, being 0.786 and 0.763, respectively. The efficiency curve of the model indicates that it captures almost 50% of the drilling sites within 10% of the area. The AUC value of the efficiency curve is 80%.

According to the statistical validation above, this combined model performs well in classifying the

known exploration targets for cobalt and also predicts new exploration areas in all six identified target areas, i.e., in central Lapland, the Peräpohja Belt, the Kuusamo Belt, the Hitura region, the Outokumpu region and southern Finland. These are the main target areas, but there are other areas with high favorability.

Co-Indications-Based Model

We also created a model that was solely based on till geochemical anomalies, exploration drilling and field observations (cobalt-bearing boulders). We first combined zinc, nickel, iron, cobalt, copper and gold from a till geochemical survey, applying the “fuzzy gamma” operator. Then, we used the “fuzzy gamma” operator to combine proximity to cobalt-bearing boulders and proximity to drilling sites with assayed samples containing over 500 ppm cobalt. We formed a random subset of the drill core dataset so that we had 80% of the data for the training and 20% left for validation. Finally, these two intermediate results were combined using the “fuzzy gamma” operator into a prospectivity map (Fig. 13). The AUC values of ROC validations using random and drilling sites are 0.801 and 0.766, respectively. The model captures almost 50% of the drilling sites within 10% of the area.

This model also performs well in classifying the validation sites and predicts targets especially in

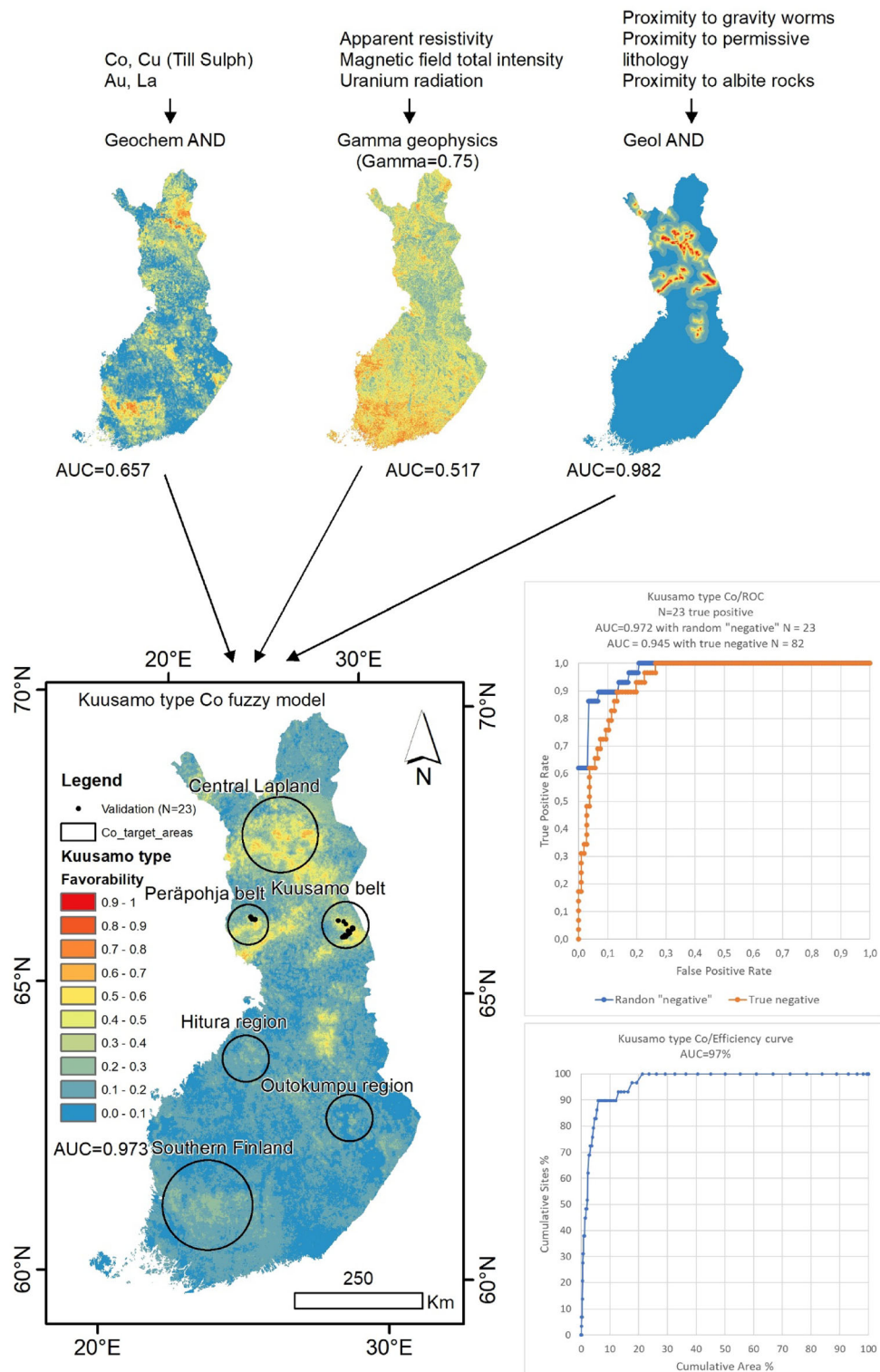


Figure 11. Kuusamo-type Co fuzzy overlay mineral prospectivity model.

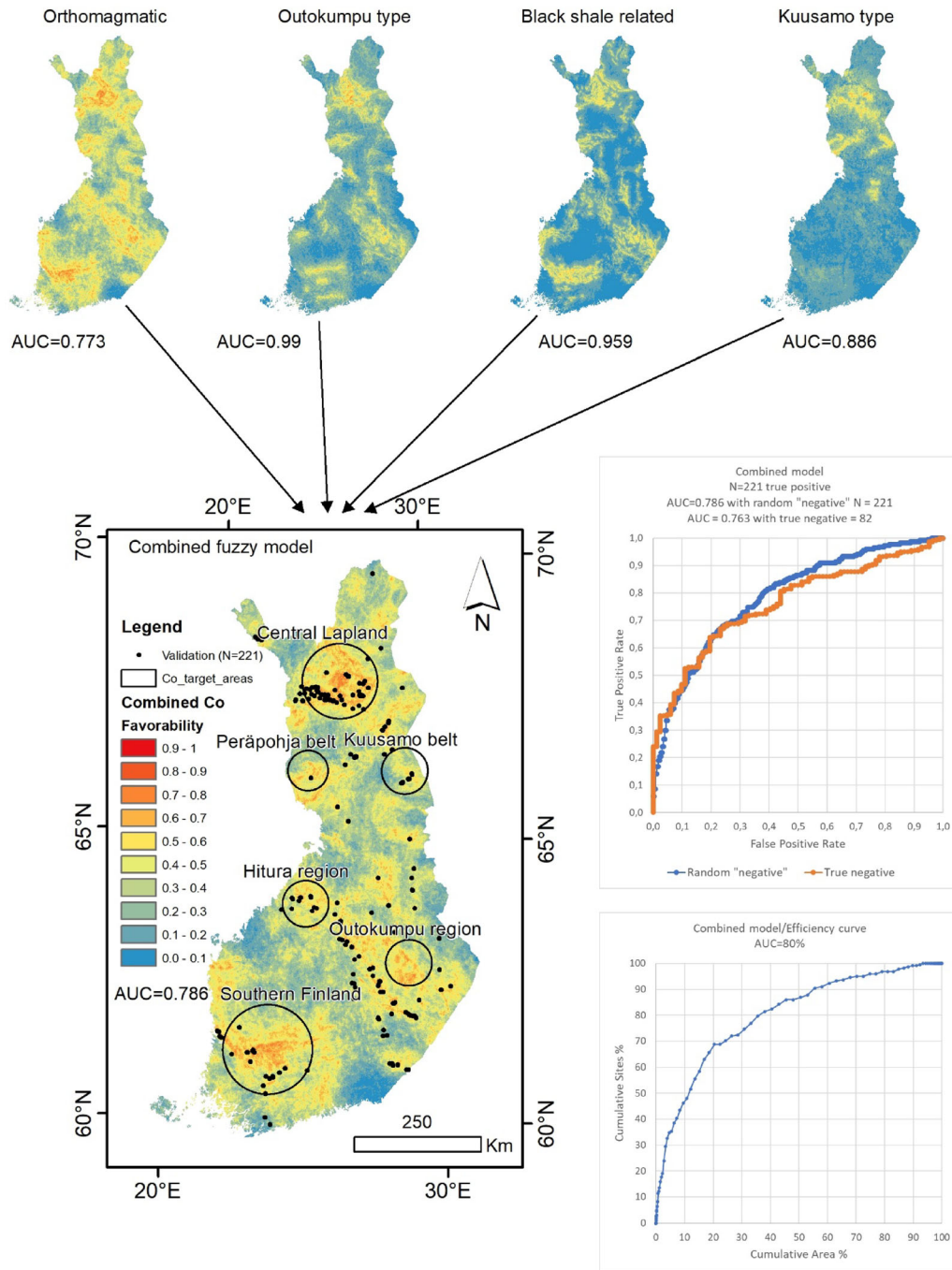


Figure 12. Combined Co fuzzy overlay mineral prospectivity model.

central Lapland, the Peräpohja Belt, the Hitura region, the Outokumpu region and southern Finland (Fig. 13). Furthermore, this model indicates some areas outside of these main target areas.

Comparison of Models

Comparison between the individual mineral systems-based models (Figs. 8, 9, 10 and 11) is not meaningful, but we briefly compared the combined

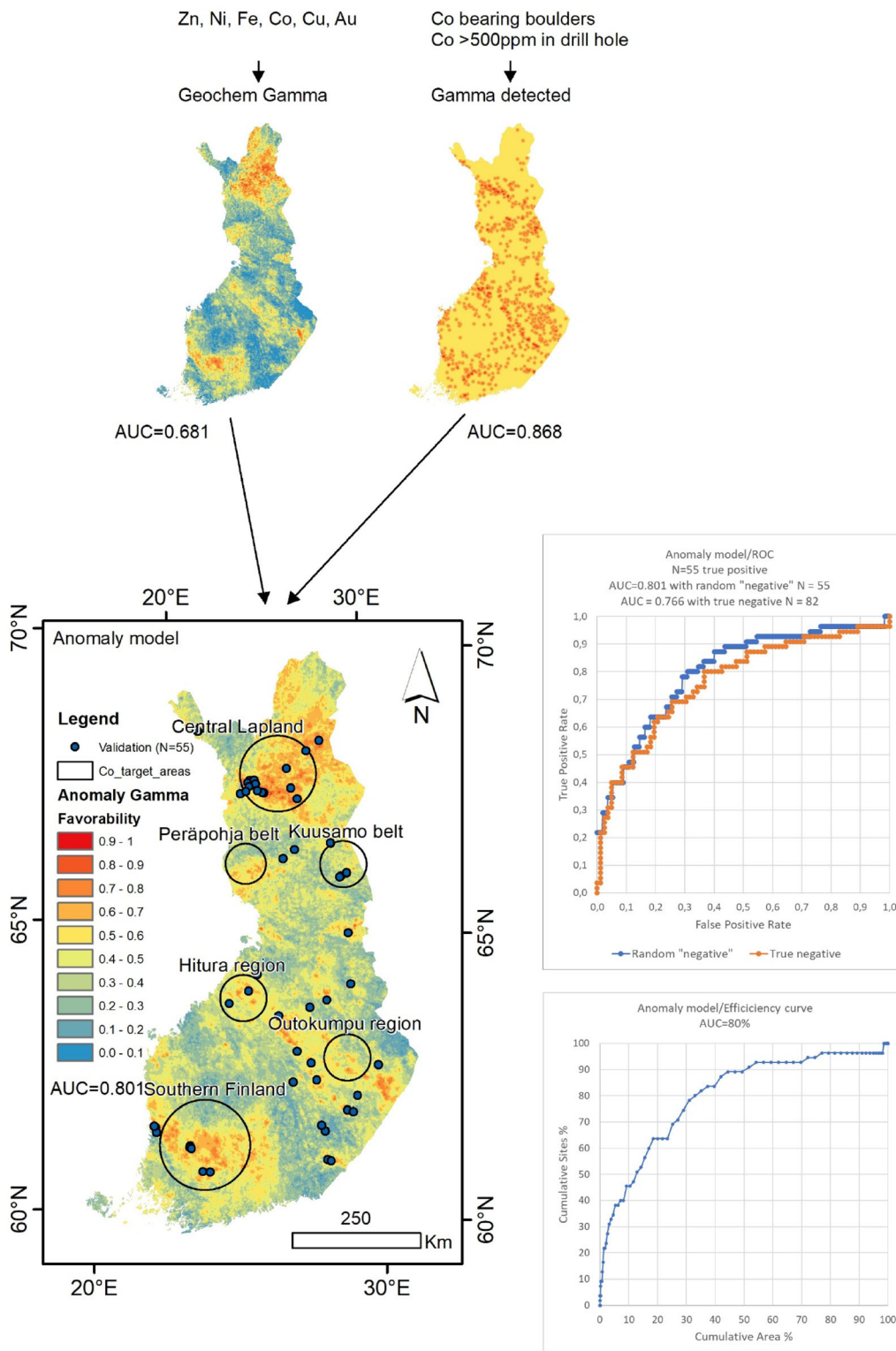


Figure 13. Anomaly-based fuzzy overlay mineral prospectivity model.

model (Fig. 12) with the anomaly model (Fig. 13). The comparison was performed by calculating the mean prospectivity value (i.e., the fuzzy membership value of the final prospectivity map for both models) within the exploration permit areas using the zonal statistics function in ArcGIS. This function extracts cell values from the value raster for all cells that fall within each zone within the exploration permit areas. We were then able to calculate statistics within these areas. The results of these measurements indicate that these models have an almost identical correlation with the current exploration activity. The mean prospectivity score is 0.52 for both, and the range is roughly from 0.3 to 0.9. The exploration permit areas thus also cover low prospectivity areas, but as can be seen from the frequency distribution graphs (Fig. 14A and B), the combined model is slightly more focused on classes above 0.5, whereas in the anomaly model, the exploration permits cover a much wider range of classes. The five black open circles in Figure 14 highlight the areas that have active exploration for cobalt based on exploration permits. All these exploration areas fall within the high favorability areas in both the combined model and the anomaly model. These areas are the Central Lapland Belt, Peräpohja Belt, Kuusamo Belt, Hitura region and Outokumpu region. When we compare these maps with the individual mineral systems-based prospectivity maps, we can see that within the Central Lapland Belt, most of the mineral occurrences containing significant amounts of cobalt are orthomagmatic, but all the models indicate that this area is highly favorable for cobalt exploration.

DISCUSSION

Prospectivity modeling for cobalt is challenging, as this commodity tends to be a by-product and not the main commodity of “*specific*” mineral deposits (Mudd et al., 2013). However, as several deposit types carry significant amounts of cobalt, we considered it feasible to conduct an analysis in which we first constructed separate mineral systems-based mineral prospectivity models and then finally combined these models instead of trying to construct a single model for cobalt prospectivity. In this way, we were able to incorporate to a certain degree the “*mineral systems approach*” (Wyborn et al., 1994; McCuaig et al., 2010) into prospectivity modeling when we used proxies for critical parameters from

each of these different systems. The use and combination of several mineral systems with a restricted number of known mineral deposits available for model training forced us to apply a knowledge-driven approach, and we selected the fuzzy logic overlay, which is indeed a flexible way to conduct this type of exercise. Previous attempts to model cobalt prospectivity within Europe, including our study area, have been conducted by Bertrand et al. (2021) using the cell-based association (CBA) method with 10 by 10 km cells covering the whole of Europe, and the data source was the 1:1.5 million scale geological map of Europe. The spatial resolution in the current study was significantly higher, as we used high-resolution airborne geophysics and several products derived from the 1:200,000 scale geological map. As noted by Lindsay et al. (2016), the use of the generalized mineral systems approach also aims to reduce the level of subjectivity in knowledge-driven mineral prospectivity modeling by including mineral systems modeling in the prospectivity modeling procedure. Lindsay et al. (2022) constructed multiple separate conceptual prospectivity models and concluded that although the five models produced in their study yielded implicitly diverse estimates for mineral potential, after combining these prospectivity models into a “*cumulative*” estimate of favorability, a robust prospectivity model for Fe ore mineralization was created.

The central Lapland area was found to be favorable for all the mineral deposit types modeled in this study (Figs. 8, 9, 10, 11 and 12) and was also favorable in the anomaly model (Fig. 13). Based on the Finnish mining registry, it is also currently one of the most active exploration areas. Within central Lapland, there are known orthomagmatic deposits, such as the Kevitsa mine (Santaguida et al., 2015) and Sakatti deposit (Brownscombe et al., 2015). There are no known Outokumpu-type deposits, but the area appears to be favorable for this deposit type, and there are indications of ophiolite sequences within the Central Lapland Greenstone Belt (Hanski, 1997). Several known atypical orogenic gold deposits with an elevated Co content have been found within the central Lapland area (Holma and Keinänen, 2007; Vasilopoulos et al., 2021), as well as other atypical orogenic gold deposits without enriched cobalt (Molnár et al., 2017b; Molnár, 2019). Based on these and other observations (Eilu et al., 2007; Patten et al., 2022) on cobalt enrichment within orogenic gold deposits in central

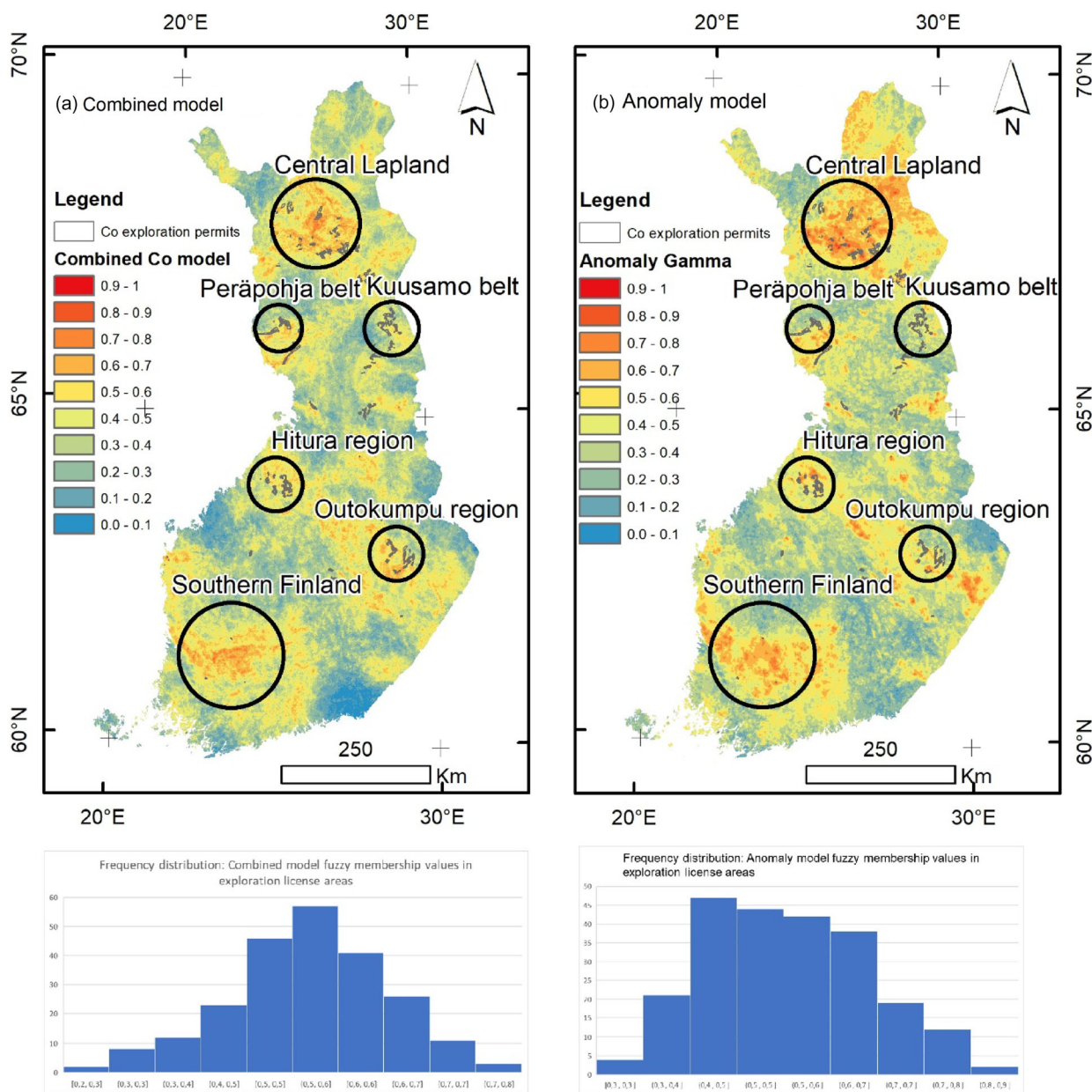


Figure 14. Comparison of the combined model (A) and the anomaly model (B).

Lapland, we consider this area to also be potential for this deposit type.

The Peräpoja Belt is potential for the orthomagmatic type (Fig. 8) and Kuusamo type of deposits (Fig. 11), and it appears to also be potential in the anomaly model (Fig. 13). So far, the most advanced exploration project has been conducted by Mawson Finland Oy on an atypical orogenic gold deposit in the Rajapalot target area (Mawson Gold

Ltd., 2022). The Kuusamo Belt appears to be potential solely for atypical orogenic gold deposits, i.e., Kuusamo-type deposits carrying cobalt.

Further south, in the Hitura region, the most common deposit type is orthomagmatic (Fig. 8), and it is the only type that becomes favorable in the models constructed in this study, in addition to the anomaly model (Fig. 13). The closed Ni-Cu Hitura mine produced 544 t of cobalt during its mining

history from the 1960s to 2013 (Törmänen and Tuomela, 2021).

The Outokumpu region appears favorable for orthomagmatic-type deposits (Fig. 8) and in the Outokumpu-type model (Fig. 9) and the anomaly model. Within this area, there are many closed Ni–Cu–Co mines, and active exploration is ongoing.

The southern Finland area is favorable for all other deposit types except the Kuusamo type examined in this study. It is also the only area that is not currently under active cobalt exploration (Fig. 14).

We used ROC validation and success rate curve diagrams to estimate the predictive performance of the prospectivity models and their ability to capture known deposits or cobalt occurrences within the study area. This provides a realistic measure of the quality of the modeling and the reliability of the results. Validation of spatial models is an essential task and often involves the selection of “*true negative*” sites that represent locations known to be barren. In this study, we tested this by comparing the results using random locations, as suggested by Nykänen et al. (2017), vs. when using another deposit type as a “*true negative*” (Nykänen, 2008), which in our case was a combination of industrial mineral deposits and lithium pegmatites. It appeared that the “*true negative*” sets resulted in somewhat more conservative AUC scores compared to the use of random locations. The difference was not always huge and some of the models yielded almost identical results. However, it is advisable to use “*true negative*” sites whenever they are available, as random negatives appear to return AUC values that are slightly too optimistic. In cases where “*true negative*” sites are unavailable, one can still safely use the random negatives, because the difference between these two is only marginal, as can be seen in the validation graphs in Figures 8, 9, 10, 11, 12 and 13.

SUMMARY AND CONCLUSIONS

This study combined four separate mineral systems-based prospectivity models into a single prospectivity model for cobalt within Finland. We also constructed an anomaly-based prospectivity model using till geochemical anomalies, field observations of cobalt-bearing boulders and outcrops, and assayed drill cores containing over 500 ppm cobalt.

The main conclusions of this study are:

1. The combination of various mineral systems models for cobalt prospectivity mapping is a valid approach;
2. A mineral systems-based model yields more focused targets compared to an anomaly-based model; and
3. ROC validation using true negative sites (e.g., other mineral deposits) results in more conservative AUC values than random negative sites.

ACKNOWLEDGMENTS

This study was funded by the Geological Survey of Finland.

FUNDING

Open Access funding provided by Geological Survey of Finland (GTK, GTK Mintec).

DECLARATIONS

Conflict of Interest The authors have no known competing interests to declare that are relevant to the content of this article.

OPEN ACCESS

This article is licensed under a Creative Commons Attribution 4.0 International License, which permits use, sharing, adaptation, distribution and reproduction in any medium or format, as long as you give appropriate credit to the original author(s) and the source, provide a link to the Creative Commons licence, and indicate if changes were made. The images or other third party material in this article are included in the article’s Creative Commons licence, unless indicated otherwise in a credit line to the material. If material is not included in the article’s Creative Commons licence and your intended use is not permitted by statutory regulation or exceeds the permitted use, you will need to obtain permission directly from the copyright holder. To view a copy of this licence, visit <http://creativecommons.org/licenses/by/4.0/>.

REFERENCES

- Abedi, M., & Norouzi, G. H. (2012). Integration of various geophysical data with geological and geochemical data to determine additional drilling for copper exploration. *Journal of Applied Geophysics*, 83, 35–45.
- Airo, M.-L. (Ed.). (2005). *Aerogeophysics in Finland 1972–2004: Methods, system characteristics and applications* (p. 197). Geological Survey of Finland. Special paper 39.
- Airo, M.-L. (2007). Application of aerogeophysical data for gold exploration: Implications for Central Lapland greenstone belt. In J. Ojala (Ed.), *Gold in the Central Lapland greenstone belt, Finland* (pp. 171–192). Geological Survey of Finland. Special paper 44.
- An, P., Moon, W. M., & Rencz, A. (1991). Application of fuzzy set theory to integrated mineral exploration. *Canadian Journal of Exploration Geophysics*, 27, 1–11.
- Barnes, S. J., Staude, S., Vaillant, M. L., Pinã, R., & Lightfoot, P. C. (2018). Sulfide-silicate textures in magmatic Ni-Cu-PGE sulfide ore deposits: Massive, semi-massive and sulfide-matrix breccia ores. *Ore Geology Reviews*, 101, 629–651.
- Bedrock of Finland – DigiKP. (2018). *Digital map database* [Electronic resource]. Espoo: Geological Survey of Finland Metadata. Retrieved 5 August 2022 from https://tupa.gtk.fi/paikkatieto/meta/bedrock_of_finland_1m.html.
- Bertrand, G., Sadeghi, M., de Oliveira, D., Tourliere, B., Arvanitidis, N., Gautneb, H., Gloaguen, E., Törmänen, T., Reginiussen, H., Pereira, A., & Quental, L. (2021). *Mineral prospectivity mapping for critical raw materials at the European scale with the CBA method* (pp. 83–86). Geological Survey of Finland, Open File Research Report 57, Mineral Prospectivity and Exploration Targeting-MinProXT 2021 Webinar. Retrieved 20 December 2022 from https://tupa.gtk.fi/raportti/arkisto/57_2021.pdf.
- Bonham-Carter, G. F. (1994). *Geographic information systems for geoscientists: Modelling with GIS* (p. 398). Pergamon.
- Bonham-Carter, G. F., Agterberg, F. P., & Wright, D. F. (1989). Weights of evidence modelling: A new approach to mapping mineral potential. In F. P. Agterberg & G. F. Bonham-Carter (Eds.), *Statistical applications in the earth sciences* (pp. 171–183). Geological Survey of Canada. Paper 89-9.
- Brownscombe, W., Ihlenfeld, C., Coppard, J., Hartshorne, C., Klatt, S., Siikaluoma, J. K., & Herrington, R. J. (2015). Chapter 3.7—The sakatti Cu-Ni-PGE sulfide deposit in northern Finland. In W. D. Maier, R. Lahtinen, & H. O'Brien (Eds.), *Mineral deposits of Finland* (pp. 211–252). Elsevier. <https://doi.org/10.1016/B978-0-12-410438-9.00009-1> ISBN 9780124104389.
- Carranza, E. J. M. (2008). Geochemical anomaly and mineral prospectivity mapping in GIS. In *Handbook of exploration and environmental geochemistry* (vol. 11). Elsevier.
- Carranza, E. J. M. (2009). Controls on mineral deposit occurrence inferred from analysis of their spatial pattern and spatial association with geological features. *Ore Geology Reviews*, 35, 383–400.
- Carranza, E. J. M., & Hale, M. (2001a). Logistic regression for geologically constrained mapping of gold potential, Baguio district, Philippines. *Exploration and Mining Geology*, 10, 165–175.
- Carranza, E. J. M., & Hale, M. (2001b). Geologically-constrained fuzzy mapping of gold mineralization potential, Baguio district, Philippines. *Natural Recourses Research*, 10, 125–136.
- Carranza, E. J. M., & Hale, M. (2002). Spatial association of mineral occurrences and curvilinear geological features. *Mathematical Geology*, 34, 203–221.
- Carranza, E. J. M., & Laborte, A. G. (2015). Random forest predictive modeling of mineral prospectivity with small number of prospects and data with missing values in Abra (Philippines). *Computers and Geosciences*, 74, 60–70.
- Carranza, E. J. M., & Laborte, A. G. (2016). Data-driven predictive modeling of mineral prospectivity using random forests: a case study in Catanduanes Island (Philippines). *Natural Recourses Research*, 25, 35–50.
- Carranza, E. J. M., Woldai, T., & Chikambwe, E. M. (2005). Application of data-driven evidential belief functions to prospectivity mapping for aquamarine-bearing pegmatites, Lundazi District, Zambia. *Natural Recourses Research*, 14, 47–63.
- Chung, C. F., & Fabbri, A. G. (2003). Validation of spatial prediction models for landslide hazard mapping. *Natural Hazards*, 30, 451–472.
- Eckstrand, O. R., & Hulbert, L. J. (2007). Magmatic nickel-copper-platinum group element deposits. In W. D. Goodfellow (Ed.), *Mineral deposits of Canada: A synthesis of major deposit types, district metallogeny, the evolution of geological provinces, and exploration methods* (pp. 205–222). Geological Association of Canada, Mineral Deposits Division, Special Publication No. 5.
- Eilu, P. (2015). Chapter 51.—Overview on gold deposits in Finland. In W. D. Maier, R. Lahtinen, & H. O'Brien (Eds.), *Mineral deposits of Finland* (pp. 377–410). Elsevier.
- Eilu P., Pankka H., Keinänen V., Kortelainen V., Niiranen T., & Pulkkinen E. (2007). Characteristics of gold mineralisation in the greenstone belts of northern Finland. In V. J. Ojala (Ed.), *Gold in Central Lapland greenstone belt* (pp. 57–106). Geological Survey of Finland. Special Paper, 44, 31 figures, one table, 4 appendices.
- Elyasi, G. R., Bahroudi, A., & Abedi, M. (2019). Risk-based analysis in mineral potential mapping: Application of quantifier-guided ordered weighted averaging method. *Natural Recourses Research*, 28, 931–951.
- Fawcett, T. (2006). An introduction to ROC analysis. *Pattern Recognition Letters*, 27, 861–874.
- Geological Survey of Finland. (2016). *Mineral deposits of Finland*. <http://hakku.gtk.fi>. Accessed 3 December 2021.
- Geological Survey of Finland. (2022a). *Mineral deposits metadata*. Retrieved 5 August 2022a from https://tupa.gtk.fi/paikkatieto/meta/mineral_deposits.html.
- Geological Survey of Finland. (2022b). *ArcSDM*. Retrieved 12 August 2022b from <https://github.com/gtkfi/ArcSDM>.
- González-Álvarez, I., Porwal, A., Beresford, S. W., McCuaig, T. C., & Maier, W. D. (2010). Hydrothermal Ni prospectivity analysis of Tasmania, Australia. *Ore Geology Reviews*, 38, 168–183.
- Groves, D. I., Goldfarb, R. J., Gebre-Mariam, M., Hagemann, S. G., & Robert, F. (1998). Orogenic gold deposits: A proposed classification in the context of their crustal distribution and relationship to other gold deposit types. *Ore Geology Reviews*, 13, 7–27.
- Groves, D. I., Santosh, M., Goldfarb, R. J., & Zhang, L. (2018). Structural geometry of orogenic gold deposits: Implications for exploration of world-class and giant deposits. *Geoscience Frontiers*, 9, 1163–1177.
- Hagemann, S. G., Lisitsin, V. A., & Huston, D. L. (2016). Mineral system analysis: Quo vadis. *Ore Geology Reviews*, 76, 504–522.
- Hanski, E. (1997). The Nuttio serpentinite belt, Central Lapland: An example of Paleoproterozoic ophiolite mantle rocks in Finland. *Ofioliti*, 22, 35–46.
- Harris, D. P., Zurcher, L., Stanley, M., Marlow, J., & Pan, G. (2003). A comparative analysis of favorability mappings by weights of evidence, probabilistic neural networks, discriminant analysis, and logistic regression. *Natural Recourses Research*, 12, 241–255.

- Harris, J. R., Grunsky, E., Behnia, P., & Corrigan, D. (2015). Data- and knowledge-driven mineral prospectivity maps for Canada's North. *Ore Geology Reviews*, 71, 788–803.
- Harris, J. R., & Grunsky, E. C. (2015). Predictive lithological mapping of Canada's North using random forest classification applied to geophysical and geochemical data. *Computers and Geosciences*, 80, 9–25.
- Harris, J. R. & Sanborn-Barrie, M. (2006). Mineral potential mapping: Examples from the Red Lake Greenstone Belt, Northwest Ontario—Chapter 1. In: J. R. Harris (Ed.), *GAC special paper 44: GIS for the earth sciences* (pp. 1–21). Geological Association of Canada Special Publication, 44.
- Harris, J. R., Wilkinson, L., Heather, K., Fumerton, S., Bernier, M. A., Ayer, J., & Dahn, R. (2001). Application of GIS processing techniques for producing mineral prospectivity maps—A case study: Mesothermal Au in the Swayze greenstone belt, Ontario, Canada. *Natural Resources Research*, 10, 91–124.
- Holma, M. J., & Keinänen, V. J. (2007). The Levijärvi-Loukinen gold occurrence: An example of orogenic gold mineralisation with atypical metal association. In V. J. Ojala (Ed.), *Gold in the Central Lapland greenstone belt* (pp. 165–186). Geological Survey of Finland. Special paper, 44.
- Horn, S., Gunn, A. G., Petavratzi, E., Shaw, R. A., Eilu, P., Törmänen, T., Bjerkgård, T., Sandstad, J. S., Jonsson, E., Kountourelis, S., & Wall, F. (2021). Cobalt resources in Europe and the potential for new discoveries. *Ore Geology Reviews*, 130, 103915.
- Hronsky, J. M. A., & Groves, D. I. (2008). Science of targeting: definition, strategies, targeting and performance measurement. *Australian Journal of Earth Sciences*, 55(1), 3–12.
- Hronsky, J. M. A., & Kreuzer, O. P. (2019). Applying spatial prospectivity mapping to exploration targeting: Fundamental practical issues and suggested solutions for the future. *Ore Geology Reviews*, 107, 647–653.
- Huhtelin, T., & Sotka, P. (1994). Kylahten Vasarakankaan näytteiden kemiallinen ja mineraloginen tutkimus. Outokumpu Oy report 073/Kylahti, mineralogia/TAH,PMS/1994. 35 p. (in Finnish).
- IEA. (2021). *The role of critical minerals in clean energy transitions*. Paris: IEA. <https://www.iea.org/reports/the-role-of-critical-minerals-in-clean-energy-transitions>. Accessed 29 November 2021.
- Joly, A., Porwal, A., McCuaig, T. C., Chudasama, B., Dentith, M. C., & Aitken, A. R. A. (2015). Mineral systems approach applied to GIS-based 2D-prospectivity modelling of geological regions: Insights from Western Australia. *Ore Geology Reviews*, 71, 673–702.
- Knox-Robinson, C. M., & Wyborn, L. A. I. (1997). Towards a holistic exploration strategy: Using geographic information systems as a tool to enhance exploration. *Australian Journal of Earth Sciences*, 44(4), 453–463.
- Koistinen, T., Stephens, M. B., Bogatchev, V., Nordgulen, Ø., Wennerström, M., & Korhonen, J. (2001). *Geological map of the Fennoscandian Shield, scale 1:2 000 000*. Geological Surveys of Finland, Norway and Sweden and the North-West Department of Natural Resources of Russia.
- Konnunaho, J., Halkoaho, T., Hanski, E., & Törmänen, T. (2015). Komatiite-hosted Ni-Cu-PGE deposits in Finland. In W. D. Maier, R. Lahtinen, & H. O'Brien (Eds.), *Mineral deposits of Finland* (pp. 93–131). Elsevier.
- Kontinen, A., & Hanski, E. (2015). Chapter 9.1—The talvivaara black shale-hosted Ni-Zn-Cu-Co deposit in eastern Finland. In W. D. Maier, R. Lahtinen, & H. O'Brien (Eds.), *Mineral deposits of Finland* (pp. 557–612). Elsevier. <https://doi.org/10.1016/B978-0-12-410438-9.00022-4>.
- Korhonen, J. V., Aaro, S., All, T., Elo, S., Haller, L. Å., Kääräinen, J., Kulinich, A., Skilbrei, J. R., Solheim, D., Säävuori, H., Vaheer, R., Zhdanova, L., & Koistinen, T. (2002). Bouguer anomaly map of the Fennoscandian Shield: IGSN 71 gravity system, GRS80 normal gravity formula. Bouguer density 2670 kg/m³, terrain correction applied. Anomaly continued upwards to 500 m above ground: scale 1:2 000 000.
- Köykkä, J., Lahtinen, R., & Huhma, H. (2019). Provenance evolution of the Paleoproterozoic metasedimentary cover sequences in northern Fennoscandia: Age distribution, geochemistry, and zircon morphology. *Precambrian Research*, 331, 105364.
- Lahtinen, R., Hölttä, P., Kontinen, A., Niiranen, T., Nironen, M., Saalman, K., & Sorjonen-Ward, P. (2011). Tectonic and metallogenic evolution of the Fennoscandian Shield: Key questions with emphasis on Finland. In K. Nenonen & P. A. Nurmi (Eds.), *Geoscience for Society 125th anniversary volume* (pp. 23–33). Geological Survey of Finland. Special paper 49.
- Lahtinen, R., & Huhma, H. (2019). A revised geodynamic model for the Lapland-Kola Orogen. *Precambrian Research*, 330, 1–19.
- Lahtinen, R., Johnston, S. T., & Nironen, M. (2014). The Bothnian coupled oroclines of the Svecofennian Orogen: A Palaeoproterozoic terrane wreck. *Terra Nova*, 26, 330–335. <https://doi.org/10.1111/ter.12107>.
- Latitude 66 Cobalt. (2019). *Press release in Finnish*. <https://lat66.com/ajankohtaista/latitude-66-cobalt-kuusamon-juomasuon-kairauksen-ja-sahkomagneettisten-tutkimusten-tulokset-ovat-hyvyn-rohkaisevia-ja-vahvistivat-tarvetta-jatkotutkimuksille/>. Accessed 10 January 2023.
- Li, X., Yuan, F., Zhang, M., Jia, C., Jowitt, S. M., Ord, A., Zheng, T., Hu, X., & Li, Y. (2015). Three-dimensional mineral prospectivity modeling for targeting of concealed mineralization within the Zhonggu iron orefield, Ningwu Basin, China. *Ore Geology Reviews*, 71, 633–654.
- Lindsay, M., Aitken, A., Ford, A., Dentith, M., Hollis, J., & Tyler, I. (2016). Reducing subjectivity in multi-commodity mineral prospectivity analyses: Modelling the west Kimberley, Australia. *Ore Geology Reviews*, 76, 395–413.
- Lindsay, M. D., Piechocka, A. M., Jessell, M. W., Scalzo, R., Giraud, J., Pirot, G., & Cripps, E. (2022). Assessing the impact of conceptual mineral systems uncertainty on prospectivity predictions. *Geoscience Frontiers*, 13, 101435. <https://doi.org/10.1016/j.gsf.2022.101435>.
- Lisitsin, V. A., González-Alvarez, I., & Porwal, A. (2013). Regional prospectivity analysis for hydrothermal-remobilised nickel mineral systems in western Victoria, Australia. *Ore Geology Reviews*, 52, 100–112.
- Loukola-Ruskeeniemi, K., & Lahtinen, H. (2013). Multiphase evolution in the black-shale-hosted Ni–Cu–Zn–Co deposit at Talvivaara, Finland. *Ore Geology Reviews*, 52, 85–99.
- Lusty, P. A. J., Scheib, C., Gunn, A. G., & Walker, A. S. D. (2012). Reconnaissance-scale prospectivity analysis for gold mineralisation in the Southern Uplands-Down-Longford Terrane, Northern Ireland. *Natural Resources Research*, 21, 359–382.
- Makkonen, H. V. (2015). Nickel deposits of the 1.88 Ga Kotalahti and Vammala belt. In W. D. Maier, H. O'Brien, & R. Lahtinen (Eds.), *Mineral deposits of Finland* (pp. 253–290). Elsevier.
- Makkonen, H. V., Halkoaho, T., Konnunaho, J., Rasilainen, K., Kontinen, A., & Eilu, P. (2017). Ni (Cu-PGE) deposits in Finland—Geology and exploration potential. *Ore Geology Reviews*, 90, 667–696.
- Mawson Gold Ltd. (2022). *Rajapalot gold cobalt project PEA*. Retrieved 20 December 2022 from <https://mawsongold.com/projects/finland/rajapalot-gold-cobalt-project-pea>.
- McCuaig, T. C., Beresford, S., & Hronsky, J. (2010). Translating the mineral systems approach into an effective exploration targeting system. *Ore Geology Reviews*, 38, 128–138.

- Mihalasky, M. J., & Bonham-Carter, G. F. (2001). Lithodiversity and its spatial association with metallic mineral sites, Great Basin of Nevada. *Natural Resources Research*, 10, 209–226.
- Molnár, F. (2019). Cobalt in orogenic gold mineral systems of northern Fennoscandia. In *NEXT—Seminar on Cobalt in Orogenic Gold Mineral Systems in Northern Fennoscandian Shield, Rovaniemi, Finland. Proceedings*.
- Molnár, F., O'Brien, H., & Lahaye, Y., Kurhila, M., Middleton, A., & Johanson, B. (2017a). Multi-stage hydrothermal processes and diverse metal associations in orogenic gold deposits of the Central Lapland Greenstone Belt, Finland. In *Mineral resources to discover—14th SGA biennial meeting* (pp. 63–66).
- Molnár, F., O'Brien, H., Stein, H., & Cook, N. D. J. (2017b). Geochronology of hydrothermal processes leading to the formation of the Au–U mineralization at the Rompas prospect, Peräpohja belt, northern Finland: Application of paired U–Pb dating of uraninite and Re–Os dating of molybdenite to the identification of multiple hydrothermal events in a metamorphic terrane. *Minerals*, 7(9), 71.
- Molnár, F., Oduro, H., Cook, N. D. J., Pohjolainen, E., Takács, A., O'Brien, H., Pakkanen, L., Johanson, B., & Wirth, R. (2016). Association of gold with uraninite and pyrobitumen in the metavolcanic rock hosted hydrothermal Au–U mineralisation at Rompas, Peräpohja Schist Belt, northern Finland. *Mineralium Deposita*, 51, 681–702.
- Mudd, G. M., Weng, Z., Jowitt, S. M., Turnbull, I. D., & Graedel, T. E. (2013). Quantifying the recoverable resources of by-product metals: the case of cobalt. *Ore Geology Reviews*, 55, 87–98.
- Murphy, F.C. (2010). *Spatial analysis of gravity gradients (worms) and fault architecture in Victoria*. Geoscience Victoria 3D Victoria Report 9. Department of Primary Industries. <https://vpls.sdp.sirsidynix.net.au/client/search/asset/1017321>. Accessed 7 December 2021.
- Naldrett, A. J. (2004). *Magmatic sulfide deposits: Geology, geochemistry, and exploration*. Springer – Verlaag, p. 728.
- Naldrett, A. J. (2011). Fundamentals of magmatic sulfide deposits. In C. Li & E. M. Ripely (Eds.), *Reviews in economic geology* (vol. 17, pp. 1–50).
- Nimis, P., Zaykov, V. V., Omenetto, P., Meleketseva, IYu., Tesalina, S. G., & Orgeval, J.-J. (2008). Peculiarities of some mafic-ultramafic- and ultramafic-hosted massive sulfide deposits from the Main Uralian Fault Zone, southern Urals. *Ore Geology reviews*, 33, 49–69.
- Nykänen, V. (2008). Radial basis functional link nets used as a prospectivity mapping tool for orogenic gold deposits within the Central Lapland Greenstone Belt, Northern Fennoscandian Shield. *Natural Resources Research*, 17, 29–48.
- Nykänen, V., Groves, D. I., Ojala, V. J., Eilu, P., & Gardoll, S. J. (2008a). Reconnaissance scale conceptual fuzzy-logic prospectivity modeling for iron oxide copper–gold deposits in the northern Fennoscandian Shield, Finland. *Australian Journal of Earth Sciences*, 55, 25–38.
- Nykänen, V., Groves, D. I., Ojala, V. J., & Gardoll, S. J. (2008b). Combined conceptual/empirical prospectivity mapping for orogenic gold in the Northern Fennoscandian Shield, Finland. *Australian Journal of Earth Sciences*, 55, 39–59.
- Nykänen, V., Lahti, I., Niiranen, T., & Korhonen, K. (2015). Receiver operating characteristics (ROC) as validation tool for prospectivity models—a magmatic Ni–Cu case study from the Central Lapland greenstone belt, Northern Finland. *Ore Geology Reviews*, 71, 853–860.
- Nykänen, V., Niiranen, T., Molnár, F., Lahti, I., Korhonen, K., Cook, N., & Skyttä, P. (2017). Optimizing a knowledge driven prospectivity model for gold deposits within Peräpohja Belt, Northern Finland. *Natural Resources Research*, 57, 571–584.
- Obuchowski, N. A. (2003). Receiver operating characteristic curves and their use in radiology. *Radiology*, 229, 3–8.
- Pan, G. C., & Harris, D. P. (2000). *Information synthesis for mineral exploration*. Oxford University Press Inc.
- Parkkinen, J. (1997). An outline of the history of exploration and mining in the Outokumpu district. In K. Loukola-Ruskeeniemi & P. Sorjonen-Ward (Eds.), *Research and exploration—Where do they meet? 4th Biennial SGA meeting, August 11–13, 1997, Turku, Finland. Excursion guidebook A4: Ore deposits in eastern Finland, Guide 42* (pp. 27–28). Geologian tutkimuskeskus.
- Patten, C. G. C., Molnár, F., Pitcairn, I. K., Kolb, J., Mertanen, S., & Hector, S. (2022). Multi-source and multi-stage metal mobilization during the tectonic evolution of the Central Lapland Greenstone Belt, Finland: Implications for the formation of orogenic Au deposits. *Mineralium Deposita*, 58(3), 461–488.
- Peltola, E. (1978). Origin of Precambrian copper sulfides of the Outokumpu district, Finland. *Economic Geology*, 73, 461–477.
- Peltonen, P., Kontinen, A., Huhma, H., & Kuronen, U. (2008). Outokumpu revisited: New mineral deposit model for the mantle peridotite-associated Cu–Co–Zn–Ni–Ag–Au sulfide deposits. *Ore Geology Reviews*, 33, 559–617.
- Pohjolainen, E., Molnár, F., O'Brien, H., Huhma, H., Tiljander, M., Sorjonen-Ward, P., Lukkari, S., Johanson, B., & Talikka, M. (2017). U–Pb geochronology of monazite from the Hangaslampi gold deposit in the Paleoproterozoic Kuusamo schist belt, northern Finland: implications for dating multi-stage mineralizing events. In *Proceedings of the 14th SGA Biennial meeting* (vol. 3, pp. 1039–1042).
- Porwal, A., Carranza, E. J. M., & Hale, M. (2003a). Extended weights-of-evidence modelling for predictive mapping of base metal deposit potential in Aravalli province, western India. *Exploration and Mining Geology*, 10, 155–163.
- Porwal, A., Carranza, E. J. M., & Hale, M. (2003b). Artificial neural networks for mineral potential mapping: A case study from Aravalli Province, Western India. *Natural Resources Research*, 12, 155–171.
- Porwal, A., Carranza, E. J. M., & Hale, M. (2003c). Knowledge-driven and data-driven fuzzy models for predictive mineral potential mapping. *Natural Resources Research*, 12, 1–25.
- Porwal, A., Carranza, E. J. M., & Hale, M. (2004). A hybrid neuro-fuzzy model for mineral potential mapping. *Mathematical Geology*, 36, 803–826.
- Porwal, A., Carranza, E. J. M., & Hale, M. (2006). A hybrid fuzzy weights-of-evidence model for mineral potential mapping. *Natural Resources Research*, 15, 1–14.
- Porwal, A., González-Álvarez, I., Markwitz, V., McCuaig, T. C., & Mamuse, A. (2010). Weights-of-evidence and logistic regression modeling of magmatic nickel sulfide prospectivity in the Yilgarn Craton, Western Australia. *Ore Geology Reviews*, 38, 184–196.
- Porwal, A. K., & Kreuzer, O. P. (2010). Introduction to the special issue: Mineral prospectivity analysis and quantitative resource estimation. *Ore Geology Reviews*, 38, 121–127.
- Raic, S., Molnár, F., Cook, N., O'Brien, H., & Lahaye, Y. (2022). Application of litho-geochemical and pyrite trace element data for the determination of vectors to ore in the Raja Au–Co prospect, northern Finland. *Solid Earth*, 13, 271–299.
- Ranta, J.-P., Hanski, E., Stein, H., Goode, M., Mäki, T., & Taitvaalkoski, A. (2020). Kivilompolo Mo mineralization in the Peräpohja belt revisited: Trace element geochemistry and Re–Os dating of molybdenite. *Bulletin of Geological Society of Finland*, 92, 131–150.
- Ranta, J. P., Molnár, F., Hanski, E., & Cook, N. (2018). Epigenetic gold occurrence in a Paleoproterozoic meta-evaporitic sequence in the Rompas-Rajapalot Au system, Peräpohja belt, northern Finland. *Bulletin of the Geological Society of Finland*, 90, 69–108.

- Rasilainen, K., Eilu, P., Huovinen, I., Konnunaho, J., Niiranen, T., Ojala, J., & Törmänen, T. (2020). *Quantitative assessment of undiscovered resources in Kuusamo-type Co-Au deposits in Finland*. Geological Survey of Finland, Bulletin 410, p 32. https://tupa.gtk.fi/julkaisu/bulletin/bt_410.pdf.
- Reino, J. (1980). Vuonoksen Cu-malmin malmimineraalien koostumusvaihtelusta. Outokumpu Oy report 070/Vuonos/J Reino/1980. 8 p. (in Finnish).
- Rodriguez-Galiano, V., Sanchez-Castillo, M., Chica-Olmo, M., & Chica-Rivas, M. (2015). Machine learning predictive models for mineral prospectivity: An evaluation of neural networks, random forest, regression trees and support vector machines. *Ore Geology Reviews*, 71, 804–818.
- Salminen, R. (Ed.) (1995). Geochemical mapping in Finland in 1982–1994. In *Finnish with summary in English* (vol. 130, p. 47). Geological Survey of Finland, Report of Investigation.
- Santaguida, F., Luolavirta, K., Lappalainen, M., Ylinen, J., Voipio, T., & Jones, S. (2015). Chapter 3.6—The Kevitsa Ni-Cu-PGE deposit in the Central Lapland Greenstone Belt in Finland. In W. D. Maier, R. Lahtinen, & H. O'Brien (Eds.), *Mineral deposits of Finland* (pp. 195–210). Elsevier. <https://doi.org/10.1016/B978-0-12-410438-9.00008-X> ISBN 9780124104389.
- Schulz, K. J., Woodruff, L. G., Nicholson, S. W., Seal II, R. R., Piatak, N. M., Chandler, V. W. & Mars, J. L. (2014). Occurrence model for magmatic sulfide-rich nickel-copper-(platinum-group element) deposits related to mafic and ultramafic dike-sill complexes. USGS, Scientific Investigations Report 2010–5070–I.
- Scoates, J. S., & Mitchell, J. N. (2000). The evolution of troctolitic and high Al basaltic magmas in Proterozoic anorthosite plutonic suites and implications for the Voicey's Bay massive Ni-Cu sulfide deposit. *Economic Geology*, 95, 677–701.
- Skirrow, R. G., Murr, J., Schofield, A., Huston, D. L., van der Wielen, S., Czarnota, K., Coghlan, R., Highet, L. M., Connolly, D., Doublier, & Duan, J. (2019). Mapping iron oxide Cu-Au (IOCG) mineral potential in Australia using a knowledge-driven mineral systems-based approach. *Ore Geology Reviews*, 113, 103011.
- Slack, J. F., Causey, J. D., Eppinger, R. G., Gray, J. E., Johnson, C. A., Lund, K. I., & Schulz, K. J. (2010). *Co-Cu-Au deposits in metasedimentary rocks—A preliminary report*. U.S. Geological Survey, Open-File Report 2010–1212.
- Tapio, J., Ranta, J.-P., Cook, N. D. J., Lahaye, Y., & O'Brien, H. (2021). Paleoproterozoic Rajapalot Au-Co system associated with evaporites: Chemical composition and boron isotope geochemistry of tourmaline, and sulfur isotopes of sulfates, Peräpohja belt, northern Finland. *Precambrian Research*, 365, 106410.
- Terrafame. (2021). *Financial review 2020*. Including Board of Directors' Review and Financial Statement. March 24, 2021.
- Törmänen, T., & Tuomela, P. (2021). *Analysis of Finnish battery mineral deposits with special emphasis on cobalt*. GTK Open File Research Report 29/2021. Retrieved 20 December 2022 from https://tupa.gtk.fi/raportti/arkisto/29_2021.pdf.
- Vanhainen E. (2001). *Geology, mineralogy and geochemistry of the Fe-Co-Au-(U) deposits in the Paleoproterozoic Kuusamo Schist Belt, northeastern Finland*. Bulletin of the Geological Survey of Finland 399.
- Vasilopoulos, M., Molnár, F., O'Brien, H., Lahaye, Y., Lefebvre, M., Andre-Mayer, A.-S., Ranta, J.-P., & Talikka, M. (2021). Geochemical signatures of mineralizing events in the Juomasuo Au-Co deposit, Kuusamo belt, northeastern Finland. *Mineralium Deposita*, 56, 1195–1222.
- Wang, G., Du, W., & Carranza, E. J. M. (2017). Remote sensing and GIS prospectivity mapping for magmatic-hydrothermal base- and precious-metal deposits in the Honghai district, China. *Journal of African Earth Sciences*, 128, 97–115.
- Weihed, P., Arndt, N., Billström, K., Duchesne, J.-C., Eilu, P., Martinsson, O., Papunen, H., & Lahtinen, R. (2005). Precambrian geodynamics and ore formation: The Fennoscandian Shield. *Ore Geology Reviews*, 27, 273–322.
- Wyborn, L. A. I., Heinrich, C. A. & Jaques, A. L. (1994). Australian Proterozoic mineral systems: essential ingredients and mappable criteria. In *Proceedings Australian institute of mining and metallurgy annual conference, Melbourne* (pp. 109–115).
- Yousefi, M., Carranza, E. J. M., Kreuzer, O. P., Nykänen, V., Hronsky, J. M. A., & Mihalasky, M. J. (2021). Data analysis methods for prospectivity modelling as applied to mineral exploration targeting: State-of-the-art and outlook. *Journal of Geochemical Exploration*, 229, 106839.
- Yousefi, M., Kreuzer, O. P., Nykänen, V., & Hronsky, J. M. A. (2019). Exploration information systems—A proposal for the future use of GIS in mineral exploration targeting. *Ore Geology Reviews*, 111, 103005.
- Yousefi, M., & Nykänen, V. (2017). Introduction to the special issue: GIS-based mineral potential targeting. *Journal of African Earth Sciences*, 128, 1–4.
- Zadeh, L. A. (1965). Fuzzy sets. *Institute of Electric and Electronic Engineering, Information and Control*, 8, 338–353.
- Zhang, Z., Zhang, J., Wang, G., Carranza, E. J. M., Pang, Z., & Wang, H. (2020). From 2D to 3D modeling of mineral prospectivity using multi-source geoscience datasets, Wulong Gold District, China. *Natural Resources Research*, 29, 345–364.
- Zuo, R., & Carranza, E. J. M. (2011). Support vector machine: A tool for mapping mineral prospectivity. *Computers and Geosciences*, 37, 1967–1975.
- Zuo, R., & Wang, Z. (2020). Effects of random negative training samples on mineral prospectivity mapping. *Natural Resources Research*, 29, 3443–3455.